New relative sea-level insights into the isostatic history of the Western Mediterranean

Matteo Vacchi, Matthieu Ghilardi, Rita T Melis, Giorgio Spada, Matthieu Giaime, Nick Marriner, Thomas Lorscheid, Christophe Morhange, Francesc Burjachs, Alessio Rovere

New relative sea-level insights into the isostatic history of the Western Mediterranean

Matteo Vacchi[1,2*], Matthieu Ghilardi[3], Rita T. Melis[4], Giorgio Spada[5], Matthieu Giaime[6], Nick Marriner[7], Thomas Lorscheid[8], Christophe Morhange[3], Francesc Burjachs[9,10,11] and Alessio Rovere[8].

[1]Geography, College of Life and Environmental Sciences, University of Exeter, EX4 4RJ, Exeter, UK

[2] Dipartimento di Scienze della Terra, Università di Pisa, Via S. Maria, 53, 56126 Pisa, Italy

[3]Aix-Marseille Université, CNRS-CEREGE, UMR 7330, IRD, Collège de France, INRA Aix en Provence, France

[4]Dipartimento Scienze Chimiche e Geologiche, Università degli Studi di Cagliari, Via Trentino 51, 09127 Cagliari, Italy

[5]Università degli Studi di Urbino, Dipartimento di Scienze Pure ed Applicate (DiSPeA), Urbino, Italy

[6]Department of Geography, Durham University, South Road, Durham, DH1 3LE, UK

[7]CNRS Chrono-Environnement UMR6249, Université de Franche-Comté, UFR ST, Besançon, France

[8]University of Bremen, Marum, ZMT, D-28359, Bremen, Germany

[9]ICREA, Barcelona, Catalonia, Spain.

[10]IPHES, Institut Català de Paleoecologia Humana i Evolució Social. Campus Sescelades URV Tarragona, Catalonia, Spain.

[11]URV, Àrea de Prehistòria, Universitat Rovira i Virgili. 43002 Tarragona, Catalonia, Spain.

*m.vacchi@exeter.ac.uk

Abstract

A recent suite of Relative Sea-Level (RSL) data for the past 12 ka BP have provided new insights into the sea-level histories of the western Mediterranean region. Our analysis of the chronostratigraphic context of sea-level indicators from Spain (Catalonia, Balearic Islands and Gulf of Valencia), France (Corsica Island) and Italy (Sardinia Island) has yielded 163 new sea-level index and limiting points. These data have considerably enhanced previous RSL compilations, in addition to improving the quality of spatio-temporal sea-level reconstructions and our capacity to estimate isostatic-related vertical motions in the western Mediterranean basin. The glacial and hydro-isostatic adjustment (GIA) pattern elucidated by the new database shows discrepancy with respect to those predicted by the available GIA models. In particular, the

new results underscore a non-coherent isostatic response of the central portion of the western Mediterranean, with the Balearic Islands manifesting significant departures from the sea-level histories of Corsica, Sardinia and, more generally, along most of the western Mediterranean coast. Our results are a crucial contribution to defining both the pattern and the magnitude of the isostatic signal along the western Mediterranean coast. In fact, vertical isostatic motions represent a key to better assess any possible post-industrial acceleration in sea-level rise and to define future scenarios of coastal inundation in the context of global change.

Keywords

Sea-level changes; isostatic adjustment; vertical crustal motion; Holocene; Mediterranean Sea

1. Introduction

Understanding how changing ice volumes have contributed to sea-level rise in the past can provide insights into the sensitivity of ice sheets to future warmer conditions, and constrain physical models used to project ice-sheet response to future climate change (e.g., Kopp et al., 2009; Dutton et al., 2015; Purcell et al., 2016). Glacial and hydro-isostatic adjustment (GIA) constitutes an important driver of past, present and future sea-level variability (e.g. Milne et al., 2009; Gehrels et al., 2011; Khan et al., 2015). For this reason, a major focus of current sea-level research is the continuous improvement of GIA geophysical models in an attempt to provide more accurate constraints for future sea-level scenarios (e.g. Nicholls et al., 2014; Goldberg et al., 2016; Roy and Peltier, 2018). Our understanding of current rates of sea-level rise from tide gauges or satellite data (e.g. Church and White, 2006; Cazenave et al., 2014; Bonaduce et al., 2016) requires correction for GIA effects that can be quantified using observations of former sea levels (e.g. Kemp et al., 2009; Engelhart et al., 2011; Rovere et al., 2016). Holocene (i.e. the last 12.0 ka BP) Relative Sea-Level (RSL) reconstructions have frequently been used to test and calibrate GIA models over timescales longer than the instrumental record (e.g., Shennan and Horton, 2002; Engelhart et al., 2011, Bradley et al., 2016; Edwards et al., 2017; Khan et al., 2017).

According to published geophysical models (e.g. Lambeck and Purcell, 2005; Stocchi and Spada, 2007; 2009; Lambeck et al., 2011; Roy and Peltier, 2018), GIA-related deformation in the Western Mediterranean

60 is mainly controlled by water loading, which has resulted in widespread subsidence throughout much of the
61 basin at an average rate of RSL rise of ~1 mm a^{-1} over the last 6000 years. Such models were tuned with
62 RSL data from several areas, particularly from the Italian coast (e.g., Lambeck et al., 2004; 2011; Antonioli
63 et al., 2009) and the western Mediterranean (Vacchi et al., 2016). However, due to its complex tectonic
64 setting (e.g., Ferranti et al., 2006; Faccenna et al., 2014), RSL histories from the Mediterranean Sea are often
65 reported as being influenced by the Holocene activity of major faults (e.g., Stiros et al., 2000, Mastronuzzi
66 and Sansò, 2002, Scicchitano et al., 2011). This has often hampered the identification of the GIA component
67 in the RSL record. This issue is even more complex in those coastal regions located at the mouth of major
68 Mediterranean rivers (e.g., Amorosi et al., 1999; 2013; Vella et al., 2005; Marriner et al., 2012a), where the
69 RSL record is strongly affected by long-term subsidence induced by sediment loading and compaction.
70 The aim of this study is to improve the quality of spatio-temporal sea-level reconstructions along a large
71 portion of the Mediterranean coast of Spain (Catalonia coast, Balearic Islands and Gulf of Valencia, figure
72 1), Corsica (France) and Sardinia (Italy), the third and second largest islands of the western Mediterranean
73 Sea, respectively (figure 1). These regions are generally located far from major tectonic boundaries (e.g.
74 much of the northern Spanish Mediterranean coast, figure 1). Furthermore, Balearic, Corsica and Sardinia
75 Islands are located in the centre of the basin, where GIA models predict a maximum hydro-isostatic
76 contribution (e.g., Lambeck and Purcell, 2004; Stocchi et al., 2007; Roy and Peltier, 2018). In all the five
77 regions, conflicting sea-level histories (see section 3), in addition to poor data quality or a paucity of Sea
78 Level Index Points (SLIPs, Shennan et al., 2015), have hindered the construction of robust RSL histories
79 and, as a result, a clear understanding of the isostatic contribution (Vacchi et al., 2016). However, a
80 significant number of new studies has been published since 2016 for these regions (see section 3). We
81 critically reviewed these recently published studies that, along with older data, allowed us to produce a new
82 suite of SLIPs and RSL limiting points following the protocol described by the International Geoscience
83 Programme (IGCP) projects 61, 200, 495 and 588 (e.g., Preuss, 1979; van de Plassche, 1982; Gehrels and
84 Long, 2007; Shennan et al., 2015). We subsequently compared the reconstructed RSL histories with the
85 predictions based on the ICE-6G (VM5a) GIA model (Peltier et al., 2015) to visualize and discuss the spatio-
86 temporal variability of the isostatic response in the Western Mediterranean.
87

2. Study area

The study area encompasses a large portion of the Western Mediterranean basin, at latitudes between ~ 39.0° N and ~43.0° N and longitudes between ~ -0.5° E and ~ 9.5° E (figure 1). The area is characterized by a microtidal regime, with tidal ranges typically not exceeding 0.45 m (Tsimplis et al., 1995).

The long record of historical seismicity, coupled with on-going crustal deformation, contributed to define the neotectonic framework of the Western Mediterranean (e.g. Faccenna et al., 2004; Serpelloni et al., 2007; Noquet, 2012). Two small oceanic basins (the Tyrrhenian and the Liguro-Provençal back-arc basins) lie on the Nubia-Eurasia convergent margin and are separated by the Corsica-Sardinia rigid continental block (e.g. Vernant et al., 2010; Faccenna et al., 2014). Some parts of the back-arc basin margins are undergoing active compressional tectonics along the east-Alboran, Algerian, and south-Tyrrhenian margins (Billi et al., 2011; Serpelloni et al., 2013). The south-Tyrrhenian compressional domain extends to northeast Sicily, while the Tyrrhenian side of the Calabrian Arc and central-southern Apennines are dominated by extension (figure 1; e.g., Ferranti et al., 2006; Faccenna et al., 2014). In these coastal areas, a major tectonic influence on the Holocene RSL evolution has often been reported (e.g., Ferranti et al., 2010; Scicchitano et al., 2011). By contrast, tectonic stability characterizes much of the Tyrrhenian and Liguro-Provençal basin (e.g. Ferranti et al., 2006; Billi et al., 2011, Nocquet, 2012). All of the coastal sectors discussed in this paper lie within areas characterised by a minimal or negligible tectonic influence on the late-Quaternary RSL evolution (e.g., Ferranti et al., 2006; Lorscheid et al., 2017; Stocchi et al., 2018). Absence of historical seismicity characterizes much of the Spanish regions included in the database (regions 1, 2 and 3, figure 1). One possible exception is the Valencia coastal plain, where weak seismic activity (< 5.0 M) is reported (Olivera et al., 1992; Anzidei et al., 2014). Both Corsica (France) and Sardinia (Italy) (regions 4 and 5, figure 1) are widely acknowledged to be amongst the most tectonically stable areas of the Mediterranean, with the absence of significant historical seismicity (Nocquet, 2012). In addition, Ferranti et al. (2006) defined negligible vertical motions during the last ~ 125 ka BP according to the present elevation of the last interglacial shoreline.

3. Previous sea-level compilations and recent sources of the RSL datapoints

115 A review of the available RSL data at the Western Mediterranean scale (Vacchi et al., 2016) allowed us to
116 constrain coastal areas where Holocene RSL histories were conflicting, of low quality or almost non-
117 existent. For the Catalonia coast, extending along the northernmost portion of the Spanish Mediterranean
118 coast (region 1, figure 1), previous data included beachrock samples and lagoonal data, the current positions
119 of which have been significantly affected by sediment compaction, especially during the mid to late-
120 Holocene (Somoza et al., 1998, Roqué Pau and Pallí Buxó, 1997; Gámez Torrent, 2007; Vacchi et al., 2016).
121 Recent investigations on the Barcelona and Empúries coastal plains (Daura et al., 2016; Ejarque et al., 2016),
122 in the Ebro Delta (Cearreta et al., 2016) and on remains of seagrass palaeo-soils (*Posidonia oceanica* mats,
123 López-Merino et al., 2017) provided useful new data to help to evaluate the RSL history of the area. The
124 Vacchi et al. (2016) review did not include a Holocene RSL curve for the Balearic Islands (region 2, figure
125 1). This was mainly due to the very limited amount of RSL data in the area. However, recent investigations
126 performed in Mallorca and Menorca (Burjachs et al., 2017, Giaime et al., 2017) coupled with the sparse
127 older data (Fornós et al., 1998, Yll et al., 1999) allowed us to comprehensively reassess the RSL history of
128 this insular complex.
129 Vacchi et al. (2016) underlined the poor quality of the RSL reconstruction for the Gulf of Valencia (region 3,
130 figure 1). Large uncertainties are associated with the SLIPs and poor descriptions of the original data did not
131 allow us to robustly assess the RSL history in this area, notably for the last 6000 years. A new dataset of
132 dated estuarine facies (Carmona et al., 2016; Blázquez et al., 2017; Rodríguez-Pérez, 2018) has facilitated a
133 significant advance in the definition of the mid- to late-Holocene RSL evolution of this coastal sector.
134 RSL histories in Corsica (region 4) show some inconsistencies (Vacchi et al., 2016). Fossil fixed biological
135 indicators sampled on the northern coast of the island (Laborel et al., 1994) indicate that RSL variations
136 during the last ~4.0 ka BP did not exceed ~2 m (Vacchi et al., 2016); these data are in agreement with the
137 new RSL dataset produced by Vacchi et al. (2017) for the eastern coast of Corsica. Conversely, data obtained
138 from a series of submerged beachrocks in the Bonifacio Strait (i.e. the narrow strait dividing Corsica and
139 Sardinia, see figure 4, Nesteroff, 1984; De Muro and Orrù, 1998; Lambeck et al., 2004) show a significant
140 departure from the above-mentioned data, with an offset of up to -3 m, especially for the mid to late-
141 Holocene (Vacchi et al., 2017). Such a discrepancy is difficult to explain in terms of the tectonic setting (see
142 section 2) or compaction-related subsidence (Vacchi et al., 2016). In this database, we tried to resolve these

discrepancies by including a new RSL dataset derived from palaeoenvironmental investigations recently performed in several Corsican coastal marshes and lagoons (Currás et al., 2017; Ghilardi et al., 2017a,b; Poher et al., 2017; Vacchi et al., 2017).

Sardinia (region 5) has been widely investigated and several types of sea-level data have been used to infer the RSL evolution (De Muro and Orrù, 1998; Orrù et al., 2004; 2011; 2014; Pirazzoli, 2005; Antonioli et al., 2007, 2012; De Falco et al., 2015). These data mainly constrain the late-Holocene RSL evolution. Conversely, a larger scatter is present in the early to mid-Holocene data. This is essentially related to compaction (such as in the Cagliari coastal plain, Antonioli et al., 2007) or beachrock dating problems (Vacchi et al., 2016; 2017). Sardinia has also been the object of recent investigations (Melis et al., 2017, 2018; Palombo et al., 2017; Pascucci et al., 2018; Ruiz et al, 2018), mainly focused on multiproxy palaeo-environmental reconstructions, yielding new sea-level data in these coastal areas.

4. Production of RSL datapoints

4.1. RSL index and limiting points

Most of the SLIPs (cf. Shennan et al., 2015; Hijma et al., 2015) in the database are derived from cores in coastal and alluvial plains, coastal marshes and lagoons. In particular, lagoons (i.e. low-energy inland waterbodies that are either intermittently or continuously connected to the open sea) are very common geomorphological features on clastic Mediterranean coasts (e.g., Di Rita et al., 2011; Salel et al., 2016; Fontana et al., 2017). Here, water depth very seldom exceeds a few meters (e.g., Marco-Barba et al., 2013; Di Rita and Melis, 2013) and samples collected in lagoonal facies have often been used to assess the palaeo sea-level position (e.g., Primavera et al., 2011; Sander et al., 2015; 2016; Vacchi et al., 2017).

In this study, we produced SLIPs from sedimentary records following the recent protocol developed for the Mediterranean (Vacchi et al., 2016, table 1). This methodology has recently been applied to a number of studies focused on Mediterranean RSL reconstructions (e.g., Fontana et al., 2017; Karkani et al., 2017, 2018; Melis et al., 2017, 2018; Ruello et al., 2017; Vacchi et al., 2017, Ghilardi et al., 2018, Kaniewsky et al., 2018). The definition of the depositional facies was based on a biostratigraphic basis and, in particular, on the macro-and micro-faunal assemblages (i.e., malacofauna, foraminifera and ostracod assemblages, e.g.,

Rossi et al., 2011; Marriner et al., 2012b; 2014). The detailed description of the indicative meaning associated with the different depositional facies (table 1) is provided in Vacchi et al., (2016).

We subsequently added to the database beachrocks, fixed biological and archaeological SLIPs already present in previous RSL reconstructions for the area (Lambeck et al., 2011; Vacchi et al., 2016).

All samples that did not show a clear and robustly established relationship with the MSL were converted into limiting points (Engelhart et al., 2015; Vacchi et al., 2016). These data are extremely important in constraining the RSL position above or below a reconstructed elevation. Reconstructed RSL points must fall below terrestrial limiting points and above marine limiting points (e.g. Engelhart and Horton, 2012; Vacchi et al., 2014). In this database, marine limiting points are typically from samples deposited in the infralittoral zone and from interlaced roots and rhizomes of the marine seagrass *Posidonia oceanica* (known as *matte*, López-Merino et al., 2017). Terrestrial limiting points are typically samples deposited in freshwater swamps, fluvial environments and upper beach/foreshore deposits (table 1). Furthermore, we considered terrestrial limiting points those archaeological indicators that were theoretically above the MSL at the time of their functioning period, such as tombs and burials (Auriemma and Solinas, 2009).

4.3. Altitude of the RSL data points

For each dated SLIP, RSL is estimated by the following equation:

$$RSL_i = A_i - RWL_i \quad [1]$$

(Shennan and Horton, 2002), where A_i is the altitude and RWL_i is the reference water level of sample i, both expressed relative to the same datum; i.e. MSL in our analysis.

The total vertical uncertainty on RSL_i is mainly represented by the indicative range and by the elevation error (Shennan and Horton, 2002). In the database presented here, the latter range from ±0.05 m for sample altitudes measured using high-precision survey methods (e.g., differential GPS) to ±0.5 m when the altitude was estimated using Digital Elevation Models, such as the sites of Torregrande and Posada in Sardinia (Melis et al., 2017, 2018).

198 In line with Hijma et al. (2015), we also considered and corrected for the following potential sources of
199 additional vertical uncertainties: (1) a core stretching/shortening error (±0.15 m for rotary corers and
200 vibracorers to ±0.05 m for hand coring), (2) a sample thickness uncertainty (3) an angle of borehole
201 uncertainty, as a function of the overburden of the sample, taken in this study to be 1 %, and (4) an
202 environmental uncertainty of 0.5 m for those samples deposited in undifferentiated brackish environments
203 (Vacchi et al., 2016, see section 4.1). Due to the microtidal setting of the research area and lack of specific
204 regional studies, we did not include an uncertainty term for potential changes in the palaeo-tidal range.
205 We subdivided the SLIPs into intercalated and basal categories (Horton and Shennan, 2009). Intercalated
206 samples are those recovered from organic horizons located between clastic layers and, therefore, are subject
207 to compaction (e.g., Hijma et al., 2015). Basal lagoonal samples are recovered from sedimentary units
208 overlying incompressible substrates (rocky basements or a thick layer of coarse sand or gravel) and are
209 therefore less prone to compaction. Virtually incompressible samples are also the fossil remains of fixed
210 biological indicators, represented by fossil rims of *Lithophyllum byssoides* (Laborel et al., 1994; Vacchi et
211 al., 2016) and beachrock samples (Mauz et al., 2015).
212
213 *4.4 Chronology of sea-level data points*
214 The age of the samples was estimated using radiocarbon (^{14}C) dating of peat layers, organic material, wood,
215 plant remains, seagrass remains and marine shells. Radiocarbon ages were calibrated into sidereal years with
216 a 2σ range. All SLIPs are presented as calibrated years before present (BP), where year 0 is AD 1950
217 (Stuiver and Polach, 1977) and were calibrated using CALIB 7.1. We employed the IntCal13 and Marine13
218 (Reimer et al., 2013) datasets for terrestrial and marine samples, respectively. Where available, local
219 reservoir corrections were taken from either the Marine Reservoir Database (Reimer and Reimer, 2001) or
220 from other published values. In calibrating the samples of organic sediment, we assumed that the original
221 depositional environment was a transitional zone in the back-coastal area, influenced by fluvial processes as
222 well as marine inputs. Therefore, for sediment dates where the percentage of marine carbon was available
223 (Melis et al., 2017, 2018) a mixed IntCal13/Marine13 calibration method was applied (Di Rita et al. 2011, Di
224 Rita and Melis, 2013).

A concern with old radiocarbon ages is the correction for isotopic fractionation (Törnqvist et al., 2015) that became a standard procedure at most laboratories by the mid-1980s (Hijma et al. 2015). In the database, the majority of samples were dated after 1990 and, therefore, most are not subject to this potential source of error. For the seven ages that are affected, we followed the procedure described by Hijma et al. (2015) to correct for isotopic fractionation.

5. Prediction of RSL

The RSL calculations presented herein have been performed using the Sea Level Equation solver SELEN (https://geodynamics.org/cig/software/selen/). The program, which was first introduced by Spada and Stocchi (2007) adopting the classical GIA theory of Farrell and Clark (1976), has now been improved and includes the rotational feedbacks on sea level, according to the method outlined by Milne and Mitrovica (1998). Furthermore, following the generalised Sea Level Equation theory described by Mitrovica and Milne (2003), our calculations fully account for the horizontal migration of the shorelines, for the transition from grounded to floating ice and for time variations of the ocean function in response to sea-level variations. In our GIA runs, we adopted the recent ICE-6G_C chronology (Peltier et al., 2015), and the mantle rheological profile VM5a. The Sea Level Equation is solved to harmonic degree 256, on a global equal area grid with spacing of ~20 km.

6. Results

We assessed 169 new radiocarbon-dated RSL data points collected in the western Mediterranean Sea. We combined these new data with 78 RSL data reported in Vacchi et al. (2016). We then reconstructed the RSL histories of the 5 regions using a database comprising 165 SLIPs and 70 limiting points (appendix A). 12 data points were rejected because of i) dating problems (i.e., Bonifacio Strait beachrocks, Vacchi et al., 2017) and anomalous $\delta^{13}C$ (‰) values of the sample, ii) difficulties in the definition of the indicative meaning and iii) discrepancies in the measurements of the altitude of archaeological structures.

The newly produced RSL data points (163 SLIPs and limiting points) constitute ~68% of the present database; the number of SLIPs (figure 2A) was increased by ~58% with respect to the Vacchi et al. (2016) compilation. It has engendered a significant improvement in the assessment of the RSL histories of the

253 Western Mediterranean. The age range of the new data spans the last ~12.0 ka BP (figure 2A), with a
254 considerable increase in the number of SLIPs, notably for the mid to late-Holocene (figure 2B).
255
256 6.1. Catalonia coast (Region 1)
257 In region 1, we improved the RSL history with 15 SLIPs and 19 terrestrial limiting points spanning the last
258 ~6 ka BP (figure 3). These data, coupled with the previously available SLIPs, facilitate the reconstruction of
259 the RSL history for the last ~6 ka BP. A suite of early-Holocene SLIPs documents a rapid rise in RSL from -
260 40 ± 0.8 m at ~12.0 ka BP to -12.3 ± 0.7 m ~8.4 ka BP. In the mid-Holocene, there is a significant
261 discrepancy between the new data and some of the older SLIPs (figure 3). However, two basal SLIPs
262 robustly place the RSL position at ~-3.0 m at ~5.8 ka BP. RSL rose slowly to -2.6 ± 0.5 m at ~4.6 ka BP and
263 at -0.8 ± 0.6 m at ~2.0 ka BP. In the last 1.5 ka BP the total RSL variation was -0.1 ± 0.6 m.
264
265 6.2. Balearic Islands (Region 2)
266 The RSL record for region 2 includes 27 SLIPs and 7 limiting points (figure 3). They constrain ~9.5 ka BP
267 of RSL evolution in an area lacking any previous sea-level reconstructions. A suite of marine limiting points
268 constrains the RSL to above ~-21 m at ~9.5 ka BP, above ~-11.5 m at ~8.4 ka BP and above ~-10.8 m at
269 ~8.0 ka BP. The oldest SLIP indicates that RSL was at -6.9 ± 0.8 m at ~7.9 ka BP, followed by a continuous
270 rising rate which brought the RSL to -3.6 ± 0.8 m at ~7.2 ka BP and to -1.5 ± 0.8 m at ~6.0 ka BP when a
271 SLIP places RSL at -1.5 ± 0.8 m. Since that period, the rising trend has slowed dramatically, with total RSL
272 variation being within 1.7 m during the last 5.3 ka BP. Younger SLIPs place the RSL at -0.5 ± 1 m at ~3.5 ka
273 BP and at -0.4 ± 1 m at ~2.0 ka BP.
274
275 6.1. Gulf of Valencia (Region 3)
276 In region 3, we improved the RSL record with 12 SLIPs and 5 limiting points spanning the last ~8.2 ka
277 (figure 3). These new data, added to the previously available ones, allow us to assess the RSL history for the
278 last ~9.1 ka BP, when the oldest SLIP places the RSL at -16.1 ± 0.6 m (figure 3). RSL rose rapidly to -10.6 ±
279 0.6 m at ~8.7 ka BP, to -4.6 ± 0.5 m at ~8.2 ka BP and to -2.1 ± 0.3 at ~7.5 ka BP. Despite significant scatter,
280 younger RSL data clearly show a significant deceleration in the rising trend. At ~4.8 ka BP, one SLIP places

281 the RSL at -0.9 ± 0.3 m while the remaining data are consistent with total RSL variation not exceeding 1 m
282 in the late-Holocene period (figure 3).
283
284 6.4. Corsica Island (Region 4)
285 In region 4, we improved the RSL record with 27 SLIPs and 16 limiting points spanning the last 5.4 ka BP
286 (figure 4). These data, merged with the previously available ones, constrain a RSL history that spans the last
287 ~8.8 ka BP (figure 4). The oldest SLIPs are both beachrocks and document a progressive RSL rise from -
288 17.5 ± 1.6 m at 8.8 ka BP to -3.8 ± 0.8 m at ~5.4 ka BP. One younger lagoonal SLIP places the RSL at -1.4 ±
289 1.0 m at ~4.6 ka BP. Since this period, the RSL is robustly constrained with the new SLIPs (mainly from
290 lagoonal samples) that are in very good agreement with the previously available *Lithophyllum byssoides*
291 SLIPs. At ~4.5 and 3.5 ka BP, RSL was at -1.77 ± 0.5 and -1.1 ± 0.3 m, respectively. RSL rose slowly to -
292 0.8 ± 0.3 m at ~2.1 ka BP and the total RSL variation in the last ~1.6 ka BP was within ~0.7 m.
293
294 6.4. Sardinia Island (Region 5)
295 In region 5, we improved the RSL record with 17 SLIPs and 18 limiting points spanning the last ~7.7 ka BP.
296 These data, merged with previously available ones, shed new light on a RSL history covering the last ~11 ka
297 BP (figure 4). A suite of basal and beachrocks SLIPs documents the rapid RSL rise of the early-Holocene
298 from -45.5 ± 1.6 m at ~10.8 ka BP to -27 ± 1.1 m at ~9.4 ka BP. At the beginning of the mid-Holocene, two
299 basal SLIPs place the RSL at -8.2 ± 1.2 and at -7.4 ± 1.2 m at ~7.7 and ~7.5 ka BP, respectively. These data
300 are only partly in agreement with two terrestrial limiting points derived from Neolithic burials (~7.3 ka BP)
301 found in the Grotta Verde cave. In fact, a first limiting point constrains the RSL below ~-8 m while a second
302 one constrains the RSL ~2 m deeper (below -10 m, Figure 4). The subsequent mid-Holocene RSL evolution
303 is constrained by a suite of SLIPs placing RSL at -4.4 ± 0.8 m at ~6.0 ka BP, at -3.6 ± 0.8 m at ~5.6 ka BP
304 and finally at -2.2 ± 1.1 m at ~4.6 ka BP. The new mid-Holocene dataset shows significant discrepancy with
305 respect to the previously available SLIPs, mainly represented by the lagoonal samples from the Gulf of
306 Cagliari and the beachrocks found in the northern sector of the Island (figure 4).
307 The late-Holocene record shows significant scatter, mainly related to the large error bar of most of the
308 SLIPs. A SLIP places the RSL at -2.3 ± 1.0 m at ~3.1 ka BP. At ~2.6 ka, a marine limiting point constrains

309 the RSL above -1.1 ± 0.2 m, in agreement with a slightly younger (~2.5 ka BP) SLIP that places the RSL at -
310 1.4 ± 1.0 m. At ~2.0 ka BP, archaeological RSL datapoints (SLIPs and terrestrial) constrain the RSL to
311 between -0.6 and -1.4 m while a younger SLIP places the RSL at -0.3 ± 1.1 m at ~1.3 ka BP.
312
313 **7. Discussion**
314 The main result of our work is a new compilation of RSL data that significantly improves the reconstruction
315 of RSL histories for five Western Mediterranean regions that were previously characterized by either a
316 paucity of data or conflicting records (Vacchi et al., 2016). The newly assembled database therefore
317 constitutes an essential benchmark to evaluate RSL patterns in the western Mediterranean Sea.
318 In effect, sediment compaction significantly influenced previous RSL reconstructions, such as those recorded
319 in the Ebro and Llobregat deltas (Somoza et al., 1998; Gámez Torrent, 2007) and the Cagliari coastal plain
320 (Orrù et al., 2004; Antonioli et al., 2007). Moreover, dating problems associated with old beachrock samples
321 from sites located between Corsica and Sardinia (figure 4, Bonifacio Strait, Nesteroff, 1984; De Muro and
322 Orrù, 1998) led to poor constraints on RSL evolution, notably for the mid to late-Holocene (Vacchi et al.,
323 2017).
324 The newly assembled RSL record clearly shows a rapid rise in the early-Holocene (~12.0 to ~8.0 ka BP)
325 followed by a sudden slowdown in the rates of RSL rise in the mid-Holocene (~7.5 and ~4.0 ka BP) and,
326 finally, by minimal changes during the late-Holocene (since ~4.0 ka BP). This sudden reduction in the rising
327 rates closely mirrors the final phase of the North America deglaciation (~7.0 ka BP; Lambeck et al., 2014).
328 This Holocene sea-level behaviour is in agreement with the pattern previously reported along the tectonically
329 stable coasts of the Western Mediterranean (Vacchi et al., 2016).
330 The new record from Catalonia shows agreement with the ICE-6G (VM5a) GIA model and is comparable,
331 within errors, to the reconstructed RSL histories of the French Mediterranean coast and northwest Italy
332 (Vacchi et al., 2016). This suggests minimal variations in the isostatic pattern over much of the northern
333 coast of the western Mediterranean.
334 Similarly, the ICE-6G (VM5a) model shows agreement with the data from Corsica and Sardinia, where the
335 expanded RSL record allowed us to resolve conflicting data and to improve our ability to quantify the

maximum isostatic contribution in the western Mediterranean basin by very significantly increasing the number of SLIPs for the last ~8.0 ka BP (see details in section 7.1).

By contrast, the model underestimates the RSL position in both the Gulf of Valencia and in the Balearic Islands, especially for the mid-Holocene. However, the RSL record from Valencia cannot be considered as an ideal setting for testing GIA models, because the area is potentially affected by land-level changes related to historical seismicity (Olivera et al., 1992; Anzidei et al., 2014). Moreover, GPS vertical velocities document a general subsidence trend (≤ 2 mm a^{-1}), especially for the Valencia coastal plains (Serpelloni et al., 2013), where most of the data were collected. For this reason, the RSL record from Valencia should be used with caution because post-depositional vertical changes (either positive or negative) may have affected the current elevation of the SLIPs and limiting points.

The Balearic Islands are located far from the Mediterranean's major tectonic boundaries (Faccenna et al., 2014; Devoti et al., 2017) and have been affected by negligible historical seismicity (Nocquet, 2012) and by minimal vertical motions during the last ~125 ka BP (Dorale et al., 2010; Stocchi et al., 2018). Here, the fit between the ICE-6G (VM5a) GIA model and the geological RSL data does not appear to be completely satisfactory, especially with regards to the mid-Holocene. This raises intriguing questions and issues potentially related to GIA processes that we address in section 7.2.

7.1. New insights into the RSL evolution of Corsica and Sardinia

A variety of geophysical models (Lambeck and Purcell, 2005; Stocchi and Spada, 2007; Roy and Peltier, 2018) predict maximum GIA-related subsidence in the centre of the western Mediterranean basin and notably along the coasts of Sardinia. This assumption was questioned by Pirazzoli (2005), who, for the last two millennia, suggested a general overestimation of the predicted isostatic signal in this area. In a more recent analysis, Antonioli et al. (2007) and subsequently Lambeck et al. (2011) improved the knowledge of the RSL evolution of Sardinia by combining previously available data (Lambeck et al., 2004) with a number of archaeological RSL indicators spanning the last 2.5 ka.

These coastal archaeological structures, mainly comprising coastal quarries, harbour structures and tombs provided new points to reconstruct the RSL history of Sardinia, representing a minimal limit for the RSL position (i.e., terrestrial limiting points, Auriemma and Solinas, 2009; Morhange and Marriner, 2015). These

364 data, coupled with the new SLIPs included in the present database are not consistent with a negligible RSL
365 variation in the last 2.0 ka BP as indicated by Pirazzoli (2005). Specifically, they are consistent with a RSL
366 change greater than ~0.8 m in the last ~2.3 ka BP (Phoenician tomb found at ~-0.76 m MSL; Antonioli et al.,
367 2007). Unfortunately, the large vertical uncertainties of the new Sardinian SLIPs do not help to significantly
368 improve the quality of the late-Holocene RSL history.
369 Conversely, the new dataset for Corsica robustly corroborates the previous RSL reconstructions (Laborel et
370 al., 1994; Vacchi et al., 2017), with an entire RSL variation that has not exceeded ~1.5 m since the beginning
371 of the late-Holocene. During this period (e.g., last ~4.0 ka BP), any RSL change in tectonically stable regions
372 is entirely controlled by GIA-related subsidence (e.g., Milne et al., 2005; Engelhart et al., 2009). The new
373 dataset for Corsica suggests a relatively uniform GIA-related subsidence pattern for the whole island, with
374 rates of ~0.4 mm a^{-1} during the last 4.0 ka. Even if the magnitudes are different, current GIA models (e.g.,
375 Stocchi and Spada, 2009; Lambeck et al., 2011; Roy and Peltier, 2018) predict an increase in GIA
376 subsidence rates from Corsica to Sardinia. Unfortunately, the lack of robust SLIPs for Sardinia during the
377 last 4.0 ka BP hampers a proper assessment of this assumption, and additional investigations are therefore
378 required to improve understanding of the local late-Holocene RSL history.
379 By contrast, the new dataset for Sardinia has yielded new information to assess the mid-Holocene RSL
380 evolution of the area. As stated in the introduction, the previously available data were mainly based on
381 lagoonal samples from the Cagliari plain (probably effected by compaction, Antonioli et al., 2007) and on
382 beachrock samples mostly collected in the Bonifacio strait (Nesteroff, 1984, De Muro and Orrù, 1998),
383 which are potentially affected by apparent younger ages related to problems in the radiometric dating of bulk
384 cement more than 30 years ago (Vacchi et al., 2017). The new lagoonal SLIPs, collected from both the
385 eastern and the western coasts of the island, show a significant departure from the data previously available
386 for the Sardinian coast. In fact, the new dataset is consistent with a RSL variation that did not exceed ~9 m in
387 the last ~7.5 ka BP. This is concomitant with the Neolithic burials (~7.3 ka BP) found at ~-8.5 m in the
388 Grotta Verde cave (Antonioli et al., 1996; 2012; Guillot, 1997), but conflicts with the coeval pottery found in
389 the same cave at -10 to -11 m (Benjamin et al., 2017; Palombo et al., 2017). Exploration of this submerged
390 cave dates back to the 1970s (Lo Schiavo, 1987) and it represents one of the oldest archaeological findings
391 used to infer past sea level in the Mediterranean (Benjamin et al., 2017). However, considerable debris flow

392 is reported along the flank of the cave and several ceramic fragments were found mixed within these debris
393 down to ~-22 m (Guillot, 1997). Furthermore, lack of information on the levelling tools adopted during the
394 cave exploration makes difficult to properly assess the vertical uncertainty of these archaeological findings.
395 The large number of SLIPs produced in this paper seems to suggest that the terrestrial limiting point found at
396 -10 to -11 m may significantly underestimate the RSL position in the first portion of the mid-Holocene.
397 However, new high-resolution mapping of archaeological findings and of the stratigraphic context of the
398 Grotta Verde are imperative to shed fresh light on this important palaeo sea-level position.
399
400 *7.2. The Balearic Islands: an isostatic conundrum*
401 The new dataset from the Balearic Islands is interesting for an assessment of the GIA pattern within the
402 Mediterranean basin. This is because the maximum GIA-related subsidence of the whole Western
403 Mediterranean (with a magnitude comparable to Sardinia) is predicted in the Balearic region (Lambeck et al.,
404 2004; Lambeck and Purcell, 2005; Stocchi and Spada, 2007; Roy and Peltier, 2018, figure 5B). However,
405 comparison with the Sardinia record shows clear discrepancies with the Balearic Islands, with the RSL
406 history in the latter plotting significantly above the first one. For instance, at ~6.0 ka, RSL in the Balearic
407 Islands (figure 3) was at least ~2 m higher than in Sardinia (figure 4).
408 As already discussed above, the Balearic Islands are considered to be amongst the most tectonically stable
409 areas of the Mediterranean (Fornós et al., 2002; Dorale et al., 2010; Sàbat et al., 2011). Thus, any possible
410 tectonic movement cannot account for the observed discrepancy that is most likely related to a differential
411 GIA response in this Mediterranean sector. The RSL history of this portion of the basin may thus represent
412 an *unicuum* in the western Mediterranean, for which the entire RSL variation in the last ~6.0 ka BP is within
413 ~2.5 m. The new lagoonal data are in agreement with the RSL reconstruction proposed on the basis of
414 archaeological findings and submerged speleothems (Gràcia et al., 2003; Tuccimei et al., 2010) and provides
415 evidence that GIA-related subsidence for this sector of the Mediterranean basin was minimal.
416 In figure 5A, we compared the best estimates of RSL changes in the Balearic Islands with Sardinia, both
417 spanning the last ~8.0 ka BP. In these regions, a comparable GIA fingerprint is predicted by the available
418 models (Galassi and Spada, 2014, figure 5B).

This comparison suggests a significant offset between the two RSL records, in conflict with the GIA model predictions. Although these data need to be corroborated by additional RSL investigations, we remark that understanding the causes of the departure of the Balearic record with respect to other regions in the database is crucial in refining the geography of isostatic processes in the Mediterranean. This is, in turn, essential in (i) defining future relative sea-level rise scenarios (e.g., Church and White, 2006; Love et al., 2016) and (ii) testing the exportability of global GIA models (e.g., Roy and Peltier, 2018). Concerning the model predictions, it should be noted that the GIA models currently employed to model RSL in the Mediterranean Sea (Lambeck and Purcell, 2005; Stocchi and Spada, 2007, 2009; Roy and Peltier, 2018) are affected by a major limitation – they do not take into account the lateral variations in mantle viscosity or in the thickness of the lithosphere. From global calculations, we know that these may well affect the Earth's response to deglaciation (e.g., Spada et al., 2006).

8. Conclusions

In this paper, we produced a new dataset of RSL index and limiting points for a number of Mediterranean regions effected by minimal tectonic influence and where GIA was the major driver of RSL evolution, notably for the last 8000 years. The isostatic pattern defined from newly assembled databases shows significant disparity with respect to those predicted by present GIA models. In particular, the new data outline a non-coherent isostatic response of the central portion of the western Mediterranean, with the Balearic Islands manifesting significant departures from the RSL evolution recorded in Corsica and Sardinia. The new data presented in this work are crucial in defining the maximum magnitude of GIA contribution along the Mediterranean coast. Ongoing GIA-related vertical motions represent a key parameter to quantify any possible post-industrial acceleration in RSL rise and to define future scenarios of coastal inundation in the Mediterranean region.

Acknowledgments

This paper is dedicated to Paolo A. Pirazzoli (1939-2017), a pioneer of sea level research in the Mediterranean Sea. This paper contributes to the MOPP-Medflood (INQUA CMP 1603P) and HOLSEA (INQUA CMP 1601P) projects. Thanks are also due to the PALSEA 2 (PAGES/INQUA/WUN working

group) and IGCP Project 639 communities for the fruitful discussions during the workshops. This work was supported by the Institutional Strategy of the University of Bremen, funded by the German Excellence Initiative (ABPZuK-03/2014) and by ZMT, the Center for Tropical Marine Ecology. Finally, we thank the two anonymous reviewers for their comments that significantly improved the significance of the paper.

9. References

Amorosi, A., Bini, M., Giacomelli, S., Pappalardo, M., Ribecai, C., Rossi, V., Sammartino, I., Sarti, G. 2013. Middle to late Holocene environmental evolution of the Pisa coastal plain (Tuscany, Italy) and early human settlements. Quaternary International, 303, 93-106.

Amorosi, A., Colalongo, M. L., Fusco, F., Pasini, G., Fiorini, F. 1999. Glacio-eustatic control of continental–shallow marine cyclicity from late Quaternary deposits of the southeastern Po Plain, northern Italy. Quaternary Research, 52(1), 1-13.

Antonioli, F., Anzidei, M., Lambeck, K., Auriemma, R., Gaddi, D., Furlani, S., Orru, P., Solinas, E., Gaspari, A., Karinja, S., Kovačić, V., Surace, L. 2007. Sea-level change during the Holocene in Sardinia and in the northeastern Adriatic (central Mediterranean Sea) from archaeological and geomorphological data. Quaternary Science Reviews, 26(19), 2463-2486.

Antonioli, F., Ferranti, L., Fontana, A., Amorosi, A., Bondesan, A., Braitenberg, C., Dutton, A., Fontolan, G., Furlani, S., Lambeck, K., Mastronuzzi, G., Monaco, C., Spada, G., Stocchi, P. 2009. Holocene relative sea-level changes and vertical movements along the Italian and Istrian coastlines. Quaternary International, 206(1), 102-133.

Antonioli, F., Ferranti, L., Lo Schiavo, F. 1996. The submerged Neolithic burials of the Grotta Verde at Capo Caccia (Sardinia, Italy) implication for the Holocene sea-level rise. Memorie Descrittive del Servizio Geologico Nazionale, 52, 290-312.

Antonioli, F., Orrù, P., Porqueddu, A., Solinas, E. 2012. Variazioni del livello marino in Sardegna durante gli ultimi millenni sulla base di indicatori geo-archeologici costieri. L'Africa romana XIX, Sassari 2010, Roma 2012, pp. 2963-2972.

Anzidei, M., Lambeck, K., Antonioli, F., Furlani, S., Mastronuzzi, G., Serpelloni, E., Vannucci, G. 2014. Coastal structure, sea-level changes and vertical motion of the land in the Mediterranean. Geological Society, London, Special Publications, 388(1), 453-479.

Auriemma, R., Solinas, E. 2009. Archaeological remains as sea level change markers: a review. Quaternary International, 206(1), 134-146.

Benjamin, J., Rovere, A., Fontana, A., Furlani, S., Vacchi, M., Inglis, R. H., Galili, E., Antonioli, F., Sivan, D., Miko, S., Mourtzas, N., Felja, I., Meredith-Williams, M., Goodman-Tchernov, B., Kolaiti, E., Anzidei, M., Gehrels, R. 2017. Late Quaternary sea-level changes and early human societies in the central and eastern Mediterranean Basin: An interdisciplinary review. Quaternary International, 449, 29-57.

Billi, A., Faccenna, C., Bellier, O., Minelli, L., Neri, G., Piromallo, C., Presti, D., Scrocca, D., Serpelloni, E. 2011. Recent tectonic reorganization of the Nubia-Eurasia convergent boundary heading for the closure of the western Mediterranean. Bulletin de la Société Géologique de France, 182(4), 279-303.

Blázquez, A. M., Rodríguez-Pérez, A., Torres, T., Ortiz, J. E. 2017. Evidence for Holocene sea level and climate change from Almenara marsh (western Mediterranean). Quaternary Research, 88(2), 206-222.

Bonaduce, A., Pinardi, N., Oddo, P., Spada, G., Larnicol, G. 2016. Sea-level variability in the Mediterranean Sea from altimetry and tide gauges. Climate Dynamics, 47(9-10), 2851-2866.

Bradley, S. L., Milne, G. A., Horton, B. P., Zong, Y. 2016. Modelling sea level data from China and Malay-Thailand to estimate Holocene ice-volume equivalent sea level change. Quaternary Science Reviews, 137, 54-68.

Burjachs, F., Pérez-Obiol, R., Picornell-Gelabert, L., Revelles, J., Servera-Vives, G., Expósito, I., Yll, E. I. 2017. Overview of environmental changes and human colonization in the Balearic Islands (Western Mediterranean) and their impacts on vegetation composition during the Holocene. Journal of Archaeological Science: Reports, 12, 845-859.

Caldara, M., Simone, O. 2005. Coastal changes in the eastern Tavoliere Plain (Apulia, Italy) during the Late Holocene: Natural or anthropic?. Quaternary Science Reviews, 24(18-19), 2137-2145.

Carboni, M. G., Bergamin, L., Di Bella, L., Iamundo, F., Pugliese, N. 2002. Palaeoecological evidences from foraminifers and ostracods on Late Quaternary sea-level changes in the Ombrone river plain (central Tyrrhenian coast, Italy). Geobios, 35, 40-50.

Carmona, P., Ruiz-Pérez, J. M., Blázquez, A. M., López-Belzunce, M., Riera, S., Orengo, H. 2016. Environmental evolution and mid–late Holocene climate events in the Valencia lagoon (Mediterranean coast of Spain). The Holocene, 26(11), 1750-1765.

Cearreta, A., Benito, X., Ibáñez, C., Trobajo, R., Giosan, L. 2016. Holocene palaeoenvironmental evolution of the Ebro Delta (Western Mediterranean Sea): Evidence for an early construction based on the benthic foraminiferal record. The Holocene, 26(9), 1438-1456.

Cazenave, A., Dieng, H. B., Meyssignac, B., Von Schuckmann, K., Decharme, B., Berthier, E. 2014. The rate of sea-level rise. Nature Climate Change, 4(5), 358-361.

510 Church, J. A., White, N. J. 2006. A 20th century acceleration in global sea-level rise. Geophysical research
511 letters, 33(1).

512 Currás, A., Ghilardi, M., Peche-Quilichini, K., Fagel, N., Vacchi, M., Delanghe, D., Contreras, D., Vella, C.,
513 Ottaviani, J. C. (2017). Reconstructing past landscapes of the eastern plain of Corsica (NW Mediterranean)
514 during the last 6000years based on molluscan, sedimentological and palynological analyses. Journal of
515 Archaeological Science: Reports, 12, 755-769.

516 Daura, J., Sanz, M., Ramos, J., Riera, S., Miras, Y., Allué, E., Picornell-Gelabert, L., López-Reyes, D.,
517 Albert, R.M., Macià, L., Domènech, R., Martinell, J., Fornós, J.J., Julià, R. 2016. Palaeoenvironmental
518 record of the Cal Maurici wetland sediment archive in Barcelona (NE Iberian Peninsula) between c. 6000
519 and 4000 cal. yr BP. The Holocene, 26(7), 1020-1039.

520 De Falco, G., Antonioli, F., Fontolan, G., Presti, V. L., Simeone, S., Tonielli, R. 2015. Early cementation and
521 accommodation space dictate the evolution of an overstepping barrier system during the Holocene. Marine
522 Geology, 369, 52-66.

523 De Muro, S., Orrù, P. 1998. Il contributo delle Beach-Rock nello studio della risalita del mare olocenico. Le
524 Beach-Rock post-glaciali della Sardegna nord-orientale. Il Quaternario, 11(1), 19-39.

525 Devoti, R., D'Agostino, N., Serpelloni, E., Pietrantonio, G., Riguzzi, F., Avallone, A., Cavaliere, A.,
526 Cheloni, D., Cecere, G., D'Ambrosio, G., Franco, L., Selvaggi, G., Metois, M., Esposito, A., Sepe, V.,
527 Galvani, A., Anzidei, M. 2017. A Combined Velocity Field of the Mediterranean Region. Annals of
528 Geophysics, 60(2), 0215.

529 Di Rita, F., Melis, R. T. 2013. The cultural landscape near the ancient city of Tharros (central West
530 Sardinia): vegetation changes and human impact. Journal of Archaeological Science, 40(12), 4271-4282.

531 Di Rita, F., Simone, O., Caldara, M., Gehrels, W. R., Magri, D. 2011. Holocene environmental changes in
532 the coastal Tavoliere Plain (Apulia, southern Italy): a multiproxy approach. Palaeogeography,
533 Palaeoclimatology, Palaeoecology, 310(3), 139-151.

534 Dorale, J. A., Onac, B. P., Fornós, J. J., Ginés, J., Ginés, A., Tuccimei, P., Peate, D. W. 2010. Sea-level
535 highstand 81,000 years ago in Mallorca. Science, 327(5967), 860-863.

536 Dutton, A., Webster, J. M., Zwartz, D., Lambeck, K., Wohlfarth, B. 2015. Tropical tales of polar ice:
537 evidence of Last Interglacial polar ice sheet retreat recorded by fossil reefs of the granitic Seychelles islands.
538 Quaternary Science Reviews, 107, 182-196.

539 Edwards, R., Gehrels, W. R., Brooks, A., Fyfe, R., Pullen, K., Kuchar, J., Craven, K. 2017. Resolving
540 discrepancies between field and modelled relative sea-level data: lessons from western Ireland. Journal of
541 Quaternary Science, 32(7), 957-975.

542 Ejarque, A., Julia, R., Reed, J. M., Mesquita-Joanes, F., Marco-Barba, J., Riera, S. 2016. Coastal evolution in
543 a Mediterranean microtidal zone: Mid to Late Holocene natural dynamics and human management of the
544 Castelló lagoon, NE Spain. PloS one, 11(5), e0155446.

545 Engelhart, S. E., Horton, B. P. 2012. Holocene sea level database for the Atlantic coast of the United States.
546 Quaternary Science Reviews, 54, 12-25.

547 Engelhart, S. E., Horton, B. P., Douglas, B. C., Peltier, W. R., Törnqvist, T. E. 2009. Spatial variability of
548 late Holocene and 20th century sea-level rise along the Atlantic coast of the United States. Geology, 37(12),
549 1115-1118.

550 Engelhart, S. E., Peltier, W. R., Horton, B. P. 2011. Holocene relative sea-level changes and glacial isostatic
551 adjustment of the US Atlantic coast. Geology, 39(8), 751-754.

552 Engelhart, S. E., Vacchi, M., Horton, B. P., Nelson, A. R., Kopp, R. E. 2015. A sea-level database for the
553 Pacific coast of central North America. Quaternary Science Reviews, 113, 78-92.

554 Faccenna, C., Becker, T. W., Auer, L., Billi, A., Boschi, L., Brun, J. P., Capitanio F., Funiciello, F., Horvat,
555 F., Jolivet L., Piromallo, C., Royden, L., Rossetti, F., Serpelloni, E. 2014. Mantle dynamics in the
556 Mediterranean. Reviews of Geophysics, 52(3), 283-332.

557 Faivre, S., Bakran-Petricioli, T., Horvatinčić, N., Sironić, A. 2013. Distinct phases of relative sea level
558 changes in the central Adriatic during the last 1500 years—influence of climatic variations?.
559 Palaeogeography, palaeoclimatology, palaeoecology, 369, 163-174.

560 Farrell, W., Clark, J., 1976. On postglacial sea-level. Geophysical Journal of Royal Astronomy Society 46,
561 647–667.

562 Ferranti, L., Antonioli, F., Mauz, B., Amorosi, A., Dai Pra, G., Mastronuzzi, G., Monaco, C., Orru, P.,
563 Pappalardo, M., Radtke, U., Renda, P., Romano., P., Sanso, P., Verrubbi, V. 2006. Markers of the last
564 interglacial sea-level high stand along the coast of Italy: tectonic implications. Quaternary international, 145,
565 30-54.

566 Fontana, A., Vinci, G., Tasca, G., Mozzi, P., Vacchi, M., Bivi, G., Rossatto, S., Salvador, L., Antonioli, F.,
567 Asioli, A., Bresolin, M., Di Mario, F., Hajdas, I. 2017. Lagoonal settlements and relative sea level during
568 Bronze Age in Northern Adriatic: Geoarchaeological evidence and paleogeographic constraints. Quaternary
569 International, 439, 17-36.

570 Fornós, J. J., Gelabert, B., Ginés, A., Ginés, J., Tuccimei, P., Vesica, P. 2002. Phreatic overgrowths on
571 speleothems: a useful tool in structural geology in littoral karstic landscapes. The example of eastern
572 Mallorca (Balearic Islands). Geodinamica Acta, 15(2), 113-125.

573 Galassi, G., Spada, G. 2014. Sea-level rise in the Mediterranean Sea by 2050: Roles of terrestrial ice melt,
574 steric effects and glacial isostatic adjustment. Global and Planetary Change, 123, 55-66.

575 Gámez Torrent D., 2007. Sequence Stratigraphy as a tool for water resources management in alluvial coastal
576 aquifers: application to the Llobregat delta (Barcelona, Spain), Ph'D Thesis, Technical University of
577 Catalonia, Barcelona, pp. 177.

578 Gehrels, W. R., Dawson, D. A., Shaw, J., Marshall, W. A. 2011. Using Holocene relative sea-level data to
579 inform future sea-level predictions: An example from southwest England. Global and Planetary Change,
580 78(3), 116-126.

581 Gehrels, W.R., Long, A.J., 2007. Quaternary land-ocean interactions: sea-level change, sediments and
582 tsunami. Marine Geology 242, 169–190.

583 Ghilardi, M., Delanghe, D., Demory, F., Leandri, F., Pêche-Quilichini, K., Vacchi, M., Vella, M.A., Rossi,
584 V., Robresco, S. 2017a. Enregistrements d'événements extrêmes et évolution des paysages dans les basses
585 vallées fluviales du Taravo et du Sagone (Corse occidentale, France) au cours de l'âge du Bronze moyen à
586 final: une perspective géoarchéologique. Géomorphologie: relief, processus, environnement, 23(1), 15-35.

587 Ghilardi, M., Istria, D., Curras, A., Vacchi, M., Contreras, D., Vella, C., Dussouillez, P., Crest, Y., Guiter, F.,
588 Delanghe, D. 2017b. Reconstructing the landscape evolution and the human occupation of the Lower Sagone
589 River (Western Corsica, France) from the Bronze Age to the Medieval period. Journal of Archaeological
590 Science: Reports, 12, 741-754.

591 Ghilardi, M., Vacchiu, M., Curràa, A., Muller Celka S., Theurillat, T., Lemos, I., Pavlopoulos, K., 2018.
592 Geoarchaeology of coastal landscape along the south Euboean Gulf (Euboea Island, Greece, during the
593 Holocene. Quaternaire 29 (2), 95-120

594 Giaime, M., Morhange, C., Ontiveros, M. Á. C., Fornós, J. J., Vacchi, M., Marriner, N. 2017. In search of
595 Pollentia's southern harbour: Geoarchaeological evidence from the Bay of Alcúdia (Mallorca, Spain).
596 Palaeogeography, Palaeoclimatology, Palaeoecology, 466, 184-201.

597 Goldberg, S. L., Lau, H. C., Mitrovica, J. X., Latychev, K. 2016. The timing of the Black Sea flood event:
598 Insights from modeling of glacial isostatic adjustment. Earth and Planetary Science Letters, 452, 178-184.

599 Gràcia, F., Jaume, D., Ramis, D., Fornós, J.J., Bover, P., Clamor, B., Gual, M.A., Vadell, M. 2003. Les
600 coves de Cala Anguila (Manacor, Mallorca). II: La Cova Genovesa o Cova d'en Bessó. Espeleogènesi,
601 geomorfologia, hidrologia, sedimentologia, fauna, paleontologia, arqueologia i conservació. Endins 25: 43–
602 86.

603 Guillot, F. 1997. La grotta di Sant Elmo o" Grotta Verde" in Alghero. Revista de l'Alguer, 8(8), 81-92.

Hijma, M., Engelhart, S. E., Törnqvist, T. E., Horton, B. P., Hu, P., Hill, D. F. 2015. A protocol for a geological sea-level database. Handbook of Sea-Level Research, edited by: Shennan, I., Long, AJ, and Horton, BP, Wiley Blackwell, 536-553.

Horton, B. P., Shennan, I. 2009. Compaction of Holocene strata and the implications for relative sealevel change on the east coast of England. Geology, 37(12), 1083-1086.

Kaniewski, D., Marriner, N., Morhange, C., Vacchi, M., Sarti, G., Rossi, V., Bini, M., Pasquinucci, M., Allinne, C., Otto, T. Luce, F., 2018. Holocene evolution of Portus Pisanus, the lost harbour of Pisa. Scientific reports, 8(1), 11625.

Karkani, A., Evelpidou, N., Giaime, M., Marriner, N., Maroukian, H., Morhange, C. 2018. Late Holocene palaeogeographical evolution of Paroikia Bay (Paros Island, Greece). Comptes Rendus Geoscience, in press. doi.org/10.1016/j.crte.2018.04.004

Karkani, A., Evelpidou, N., Vacchi, M., Morhange, C., Tsukamoto, S., Frechen, M., Maroukian, H. 2017. Tracking shoreline evolution in central Cyclades (Greece) using beachrocks. Marine Geology 388, 25-37.

Kemp, A. C., Horton, B. P., Culver, S. J., Corbett, D. R., van de Plassche, O., Gehrels, W. R., Douglas, B.C., Parnell, A. C. 2009. Timing and magnitude of recent accelerated sea-level rise (North Carolina, United States). Geology, 37(11), 1035-1038.

Khan, N. S., Ashe, E., Horton, B. P., Dutton, A., Kopp, R. E., Brocard, G., Engelhart, S.E., Hill, F.F., Peltier, W.R., Vane, C.H., Scatena, F. N. 2017. Drivers of Holocene sea-level change in the Caribbean. Quaternary Science Reviews, 155, 13-36.

Khan, N. S., Ashe, E., Shaw, T. A., Vacchi, M., Walker, J., Peltier, W. R., Kopp, R.E., Horton, B. P. 2015. Holocene relative sea-level changes from near-, intermediate-, and far-field locations. Current Climate Change Reports, 1(4), 247-262.

Kopp, R. E., Simons, F. J., Mitrovica, J. X., Maloof, A. C., Oppenheimer, M. 2009. Probabilistic assessment of sea level during the last interglacial stage. Nature, 462(7275), 863-867.

Laborel, J., Morhange, C., Lafont, R., Le Campion, J., Laborel-Deguen, F., Sartoretto, S. 1994. Biological evidence of sea-level rise during the last 4500 years on the rocky coasts of continental southwestern France and Corsica. Marine Geology, 120(3-4), 203-223.

Lambeck, K., Antonioli, F., Anzidei, M., Ferranti, L., Leoni, G., Scicchitano, G., Silenzi, S. 2011. Sea level change along the Italian coast during the Holocene and projections for the future. Quaternary International, 232(1), 250-257.

Lambeck, K., Antonioli, F., Purcell, A., Silenzi, S. 2004. Sea-level change along the Italian coast for the past 10,000 yr. Quaternary Science Reviews, 23(14), 1567-1598.

636 Lambeck, K., Purcell, A. 2005. Sea-level change in the Mediterranean Sea since the LGM: model
637 predictions for tectonically stable areas. Quaternary Science Reviews, 24(18), 1969-1988.

638 Lambeck, K., Rouby, H., Purcell, A., Sun, Y., Sambridge, M. 2014. Sea level and global ice volumes from
639 the Last Glacial Maximum to the Holocene. Proceedings of the National Academy of Sciences, 111(43),
640 15296-15303.

641 Lambeck, K., Smither, C., Johnston, P. 1998. Sea-level change, glacial rebound and mantle viscosity
642 fornorthern Europe. Geophysical Journal International, 134(1), 102-144.

643 Lo Schiavo, F., 1987. Grotta Verde 1979: un contributo sul neolitico antico della Sardegna Atti della XXVI
644 Riunione Scientifica dell'Istituto Italiano di Preistoria e Protostoria, pp. 845-858

645 López-Merino, L., Colás-Ruiz, N. R., Adame, M. F., Serrano, O., Martínez Cortizas, A., & Mateo, M. A.
646 2017. A six thousand-year record of climate and land-use change from Mediterranean seagrass mats. Journal
647 of Ecology 105, (5): 1267–1278.

648 Lorscheid, T., Stocchi, P., Casella, E., Gómez-Pujol, L., Vacchi, M., Mann, T., Rovere, A. 2017. Paleo sea-
649 level changes and relative sea-level indicators: Precise measurements, indicative meaning and glacial
650 isostatic adjustment perspectives from Mallorca (Western Mediterranean). Palaeogeography,
651 Palaeoclimatology, Palaeoecology, 473, 94-107.

652 Love, R., Milne, G. A., Tarasov, L., Engelhart, S. E., Hijma, M. P., Latychev, K., ... Törnqvist, T. E. 2016.
653 The contribution of glacial isostatic adjustment to projections of sea-level change along the Atlantic and Gulf
654 coasts of North America. Earth's Future, 4(10), 440-464.

655 Marco-Barba, J., Holmes, J. A., Mesquita-Joanes, F., Miracle, M. R. 2013. The influence of climate and sea-
656 level change on the Holocene evolution of a Mediterranean coastal lagoon: Evidence from ostracod
657 palaeoecology and geochemistry. Geobios, 46(5), 409-421.

658 Marriner, N., Flaux, C., Morhange, C., Kaniewski, D. 2012a. Nile Delta's sinking past: Quantifiable links
659 with Holocene compaction and climate-driven changes in sediment supply?. Geology, 40(12), 1083-1086.

660 Marriner, N., Gambin, T., Djamali, M., Morhange, C., Spiteri, M. 2012b. Geoarchaeology of the Burmarrad
661 ria and early Holocene human impacts in western Malta. Palaeogeography, Palaeoclimatology,
662 Palaeoecology, 339, 52-65.

663 Marriner, N., Morhange, C., Faivre, S., Flaux, C., Vacchi, M., Miko, S., Dumas, V., Boetto, G., Rossi, I. R.
664 2014. Post-Roman sea-level changes on Pag Island (Adriatic Sea): Dating Croatia's "enigmatic" coastal
665 notch?. Geomorphology, 221, 83-94.

666 Morhange, C., Marriner, N. 2015. Archeological and biological relative sea-level indicators. Handbook of
667 sea-level research, 146-156.

668 Mastronuzzi, G., Sansò, P. 2002. Holocene uplift rates and historical rapid sea-level changes at the Gargano
669 promontory, Italy. Journal of Quaternary Science, 17(5-6), 593-606.

670 Mauz, B., Vacchi, M., Green, A., Hoffmann, G., Cooper, A. 2015. Beachrock: a tool for reconstructing
671 relative sea level in the far-field. Marine Geology, 362, 1-16.

672 Melis, R. T., Di Rita, F., French, C., Marriner, N., Montis, F., Serreli, G., Sulas, F., Vacchi, M. 2018. 8000
673 years of coastal changes on a western Mediterranean island: A multiproxy approach from the Posada plain of
674 Sardinia. Marine Geology 403, 93-108.

675 Melis, R. T., Depalmas, A., Di Rita, F., Montis, F., Vacchi, M. 2017. Mid to late Holocene environmental
676 changes along the coast of western Sardinia (Mediterranean Sea). Global and Planetary Change. 155, 29-41.

677 Milne, G. A., Gehrels, W. R., Hughes, C. W., Tamisiea, M. E. 2009. Identifying the causes of sea-level
678 change. Nature Geoscience, 2(7), 471-478.

679 Milne, G., Mitrovica, J., 1998. Postglacial sea-level change on a rotating Earth. Geophysical Journal
680 International 133 (1), 1–19.

681 Milne, G.A., Long, A.J., Bassett, S.E., 2005. Modeling Holocene relative sea-level observations from the
682 Caribbean and South America. Quaternary Science Reviews 24, 1183–1202.

683 Mitrovica, J.X., Milne, G.A., 2003. On postglacial sea level: I. General Theory. Geophysical Journal
684 International, 154 (2), 253–267.

685 Nesteroff, W. D. 1984. Étude de quelques grès de plage du sud de la Corse: datations 14C et implications
686 néotectoniques pour le bloc corso-sarde. Travaux de la Maison de l'Orient, 8(1), 99-111.

687 Nicholls, R. J., Hanson, S. E., Lowe, J. A., Warrick, R. A., Lu, X., Long, A. J. 2014. Sea-level scenarios for
688 evaluating coastal impacts. Wiley Interdisciplinary Reviews: Climate Change, 5(1), 129-150.

689 Nocquet, J. M. 2012. Present-day kinematics of the Mediterranean: A comprehensive overview of GPS
690 results. Tectonophysics, 579, 220-242.

691 Olivera, C., Susagna, T., Roca, A., Goula, X. 1992. Seismicity of the Valencia trough and surrounding areas.
692 Tectonophysics, 203(1-4), 99-109.

693 Orrù, P.E., Antonioli, F., Lambeck, K., Verrubbi, V. 2004. Holocene sea-level change in the Cagliari coastal
694 plain (southern Sardinia, Italy). Quaternaria Nova

695 Orrù, P.E., Mastronuzzi, G., Deiana, G., Pignatelli, C., Piscitelli, A., Solinas, E., Spanu, P., Zucca, R. 2014.
696 Sea level changes and geoarchaeology between the bay of Capo Malfatano and Piscinnì Bay (SW Sardinia)
697 in the last 4 kys. Quaternary International 336, 180-189.

Orrù, P.E., Solinas, E., Puliga, G., Deiana, G. 2011. Palaeo-shorelines of the historic period, Sant'Antioco Island, south-western Sardinia (Italy). Quaternary International 232(1), 71-81.

Palombo, M. R., Antonioli, F., Presti, V. L., Mannino, M. A., Melis, R. T., Orru, P., Stocchi, P., Talamo, S., Quarta, G., Calcagnile, L., Deiana, G., Altamura, S. 2017. The late Pleistocene to Holocene palaeogeographic evolution of the Porto Conte area: Clues for a better understanding of human colonization of Sardinia and faunal dynamics during the last 30 ka. Quaternary International, 439, 117-140.

Pascucci, V., De Falco, G., Del Vais, C., Sanna, I., Melis, R. T., Andreucci, S. 2018. Climate changes and human impact on the Mistras coastal barrier system (W Sardinia, Italy). Marine Geology, 395, 271-284.

Peltier, W. R. 2004. Global glacial isostasy and the surface of the ice-age Earth: the ICE-5G (VM2) model and GRACE. Annual Review of Earth and Planetary Science, 32, 111-149.

Peltier, W., Argus, D., Drummond, R., 2015. Space geodesy constrains ice age terminal deglaciation: the global ICE-6G_C (VM5a) model. Journal of Geophys. Research 120 (1), 450–487.

Pirazzoli, P. A. 2005. A review of possible eustatic, isostatic and tectonic contributions in eight late-Holocene relative sea-level histories from the Mediterranean area. Quaternary Science Reviews, 24(18), 1989-2001.

Poher, Y., Ponel, P., Médail, F., Andrieu-Ponel, V., Guiter, F. 2017. Holocene environmental history of a small Mediterranean island in response to sea-level changes, climate and human impact. Palaeogeography, Palaeoclimatology, Palaeoecology, 465, 247-263.

Preuss, H., 1979. Progress in Computer Evaluation of Sea Level Data within the IGCP Project no. 61. Proc. 1978 International Symposium of Coastal Evolution in the Quaternary, pp. 104–134.

Primavera, M., Simone, O., Fiorentino, G., Caldara, M. 2011. The palaeoenvironmental study of the Alimini Piccolo lake enables a reconstruction of Holocene sea-level changes in southeast Italy. The Holocene 21(4), 553-563.

Purcell, A., Tregoning, P., Dehecq, A. 2016. An assessment of the ICE6G_C (VM5a) glacial isostatic adjustment model. Journal of Geophysical Research: Solid Earth, 121(5), 3939-3950.

Reimer, P. J., Bard, E., Bayliss, A., Beck, J. W., Blackwell, P. G., Ramsey, C. B., ... Grootes, P. M. 2013. IntCal13 and Marine13 radiocarbon age calibration curves 0–50,000 years cal BP. Radiocarbon, 55(4), 1869-1887.

Reimer, P. J., Reimer, R. W. 2001. A marine reservoir correction database and on-line interface. Radiocarbon, 43(2A), 461-463.

728 Rodríguez-Pérez, A., Blázquez, A. M., Guillem, J., Usera, J. 2018. Maximum flood area during MIS 1 in the
729 Almenara marshland (Western Mediterranean): Benthic foraminifera and sedimentary record. The Holocene,
730 in press doi.org/10.1177/0959683618777069

731 Roqué Pau, C., Pallí Buxó, L. 1997. Depósitos litorales y variaciones del nivel del mar durante el Holoceno
732 en la Costa Brava (NE de Catalunya). Reunion del Cuaternario Ibérico: Asociación Española para el Estudio
733 del Cuaternario [AEQUA]: 1997: Huelva, 1997, p. 178-183.

734 Rovere, A., Stocchi, P., Vacchi, M. 2016. Eustatic and relative sea level changes. Current Climate Change
735 Reports, 2(4), 221-231.

736 Rossi, V., Amorosi, A., Sarti, G., Potenza, M. 2011. Influence of inherited topography on the Holocene
737 sedimentary evolution of coastal systems: an example from Arno coastal plain (Tuscany, Italy).
738 Geomorphology, 135(1-2), 117-128.

739 Roy, K., Peltier, W. R. (2018). Relative sea level in the Western Mediterranean basin: A regional test of the
740 ICE-7G_NA (VM7) model and a constraint on late Holocene Antarctic deglaciation. Quaternary Science
741 Reviews, 183, 76-87.

742 Ruello, M. R., Cinque, A., Di Donato, V., Molisso, F., Terrasi, F., Ermolli, E. R. 2017. Interplay between sea
743 level rise and tectonics in the Holocene evolution of the St. Eufemia Plain (Calabria, Italy). Journal of
744 Coastal Conservation, 21(6), 903-915.

745 Ruiz, J. M., Carmona, P., Gomez-Bellard, C., van Dommelen, P. 2018. Geomorphology and environmental
746 change around the Punic sites of the Terralba plain (Oristano Gulf, Sardinia, Italy). Boletin Geologico y
747 Minero, 129(1-2), 331-351.

748 Sàbat, F., Gelabert, B., Rodríguez-Perea, A., Giménez, J. 2011. Geological structure and evolution of
749 Majorca: Implications for the origin of the Western Mediterranean. Tectonophysics, 510(1), 217-238.

750 Sabatier, P., Dezileau, L., Colin, C., Briqueu, L., Bouchette, F., Martinez, P., ... Von Grafenstein, U. 2012.
751 7000 years of paleostorm activity in the NW Mediterranean Sea in response to Holocene climate events.
752 Quaternary Research, 77(1), 1-11.

753 Salel, T., Bruneton, H., Lefèvre, D. 2016. Ostracods and environmental variability in lagoons and deltas
754 along the north-western Mediterranean coast (Gulf of Lions, France and Ebro delta, Spain). Revue de
755 Micropaléontologie, 59(4), 425-444.

756 Sander, L., Fruergaard, M., Koch, J., Johannessen, P. N., Pejrup, M. 2015. Sedimentary indications and
757 absolute chronology of Holocene relative sea-level changes retrieved from coastal lagoon deposits on Samsø,
758 Denmark. Boreas, 44(4), 706-720.

759 Sander, L., Hede, M. U., Fruergaard, M., Nielsen, L., Clemmensen, L. B., Kroon, A., Johannessen, P.N.,
760 Nielsen, L.H., Pejrup, M. 2016. Coastal lagoons and beach ridges as complementary sedimentary archives
761 for the reconstruction of Holocene relative sea-level changes. Terra Nova, 28(1), 43-49.

762 Scicchitano, G., Spampinato, C. R., Ferranti, L., Antonioli, F., Monaco, C., Capano, M., Lubritto, C. 2011.
763 Uplifted Holocene shorelines at Capo Milazzo (NE Sicily, Italy): evidence of co-seismic and steady-state
764 deformation. Quaternary International, 232(1), 201-213.

765 Serpelloni, E., Faccenna, C., Spada, G., Dong, D., Williams, S. D. 2013. Vertical GPS ground motion rates
766 in the Euro-Mediterranean region: New evidence of velocity gradients at different spatial scales along the
767 Nubia-Eurasia plate boundary. Journal of Geophysical Research: Solid Earth, 118(11), 6003-6024.

768 Serpelloni, E., Vannucci, G., Pondrelli, S., Argnani, A., Casula, G., Anzidei, M., Baldi., P., Gasperini, P.
769 2007. Kinematics of the Western Africa-Eurasia plate boundary from focal mechanisms and GPS data.
770 Geophysical Journal International, 169(3), 1180-1200.

771 Shaw, T. A., Kirby, J. R., Holgate, S., Tutman, P., Plater, A. J. 2016. Contemporary salt-marsh foraminiferal
772 distribution from the Adriatic coast of Croatia and its potential for sea-level studies. The Journal of
773 Foraminiferal Research, 46(3), 314-332.

774 Shennan, I., Horton, B. 2002. Holocene land-and sea-level changes in Great Britain. Journal of Quaternary
775 science, 17(5-6), 511-526.

776 Shennan, I., Long, A.J., Horton, B.P., 2015. Handbook of Sea-Level Research. John Wiley & Sons

777 Somoza, L., Barnolas, A., Arasa, A., Maestro, A., Rees, J. G., Hernández-Molina, F. J. 1998. Architectural
778 stacking patterns of the Ebro delta controlled by Holocene high-frequency eustatic fluctuations, delta-lobe
779 switching and subsidence processes. Sedimentary Geology 117(1), 11-32.

780 Spada, G., Stocchi, P., 2007. SELEN: a Fortran 90 program for solving the ‘‘Sea Level Equation’’. Comput.
781 Geosci. 33 (4), 538–562.

782 Spada, G., Antonioli, A., Cianetti, S., Giunchi, C. 2006. Glacial isostatic adjustment and relative sea-level
783 changes: the role of lithospheric and upper mantle heterogeneities in a 3-D spherical Earth, Geophysical
784 Journal International 165 (2), 692-702

785 Stiros, S. C., Laborel, J., Laborel-Deguen, F., Papageorgiou, S., Evin, J., Pirazzoli, P. A. 2000. Seismic
786 coastal uplift in a region of subsidence: Holocene raised shorelines of Samos Island, Aegean Sea, Greece.
787 Marine Geology, 170(1), 41-58.

788 Stocchi, P., Spada, G. 2007. Glacio and hydro-isostasy in the Mediterranean Sea: Clark s zones and role of
789 remote ice sheets. Annals of Geophysics, 50(6).

790 Stocchi, P., Spada, G. 2009. Influence of glacial isostatic adjustment upon current sea level variations in the
791 Mediterranean. Tectonophysics, 474(1), 56-68.

792 Stocchi, P., Vacchi, M., Lorscheid, T., de Boer, B., Simms, A. R., van de Wal, R. S., Vermeesen, B.L.A.,
793 Pappalardo, M., Rovere, A. 2018. MIS 5e relative sea-level changes in the Mediterranean Sea: Contribution
794 of isostatic disequilibrium. Quaternary Science Reviews, 185, 122-134.

795 Stuiver, M., Polach, H.A., 1977. Reporting 14C data. Radiocarbon 19, 355–363.

796 Tornqvist, T.E., Rosenheim, B.E., Hu, P., Fernandez, A.B., 2015. Radiocarbon dating and calibration. In:
797 Long, A.J., Horton, B.P. (Eds.), Shennan, I. Wiley, Handbook of Sea-level Research, pp. 349–360.

798 Tsimplis, M. N., Proctor, R., Flather, R. A. 1995. A two-dimensional tidal model for the Mediterranean Sea.
799 Journal of Geophysical Research: Oceans, 100(C8), 16223-16239.

800 Tuccimei, P., Soligo, M., Ginés, J., Ginés, A., Fornós, J., Kramers, J., Villa, I. M. 2010. Constraining
801 Holocene sea levels using U-Th ages of phreatic overgrowths on speleothems from coastal caves in Mallorca
802 (Western Mediterranean). Earth Surface Processes and Landforms, 35(7), 782-790.

803 Vacchi, M., Ghilardi, M., Spada, G., Currás, A., Robresco, S. 2017. New insights into the sea-level evolution
804 in Corsica (NW Mediterranean) since the late Neolithic. Journal of Archaeological Science: Reports, 12,
805 782-793.

806 Vacchi, M., Marriner, N., Morhange, C., Spada, G., Fontana, A., Rovere, A. 2016. Multiproxy assessment of
807 Holocene relative sea-level changes in the western Mediterranean: sea-level variability and improvements in
808 the definition of the isostatic signal. Earth-Science Reviews, 155, 172-197.

809 Vacchi, M., Rovere, A., Chatzipetros, A., Zouros, N., Firpo, M. 2014. An updated database of Holocene
810 relative sea level changes in NE Aegean Sea. Quaternary International, 328, 301-310.

811 Vacchi, M., Rovere, A., Zouros, N., Desruelles, S., Caron, V., Firpo, M. 2012. Spatial distribution of sea-
812 level markers on Lesvos Island (NE Aegean Sea): evidence of differential relative sea-level changes and the
813 neotectonic implications. Geomorphology, 159, 50-62.

814 van de Plassche, O., 1982. Sea-level change and water-level movements in the Netherlands during the
815 Holocene. Med. Rijks Geol. Dienst. 36, 1–93.

816 Vella, C., Fleury, T. J., Raccasi, G., Provansal, M., Sabatier, F., Bourcier, M. 2005. Evolution of the Rhône
817 delta plain in the Holocene. Marine Geology, 222, 235-265.

818 Vernant, P., Fadil, A., Mourabit, T., Ouazar, D., Koulali, A., Davila, J. M., Garate, J., McClusky, S.,
819 Reilinger, R. 2010. Geodetic constraints on active tectonics of the Western Mediterranean: Implications for
820 the kinematics and dynamics of the Nubia-Eurasia plate boundary zone. Journal of Geodynamics, 49(3),
821 123-129.

822 Yll, R., Pantaleón-Cano, J., Pérez-Obiol, R.P., Roure, J. M. 1999. Cambio climático y transformación del
823 medio durante el Holoceno en las Islas Baleares. Congrés del Neolític a la Península Ibérica, Saguntum
824 Extra, 2, 45-51.

825
826
827 Figure captions
828
829 Figure 1. Spatial extent of the study area. Numbered rectangles denote the location of sea-level data for this
830 study, grouped into five regions as explained in the text. Tectonic framework of the western Mediterranean.
831 Faults are modified after Faccenna et al. (2014) and Vacchi et al. (2016).
832
833 Figure 2. A) Total plot of the 165 SLIPs used for the RSL reconstructions in the 5 regions. Red SLIPs
834 represent those produced for the present database. Grey SLIPs are those included in the Vacchi et al. (2016)
835 compilation. B) Stacked histogram of the SLIPs showing an increase in the number of SLIPs compared to
836 the Vacchi et al. (2016) compilation.
837
838 Figure 3. RSL reconstructions in Catalonia (1), the Balearic Islands (2) and Gulf of Valencia (3) regions.
839 SLIPs (boxes) are plotted as calibrated ages against change in sea level relative to present. Limiting points
840 are plotted as terrestrial or marine horizontal lines. The dimensions of boxes and lines for each point are
841 based on elevation and age errors. Black lines denote the geography of relative sea-level predictions
842 calculated using SELEN and adopting the ICE-6G (VM5a) GIA model (see section 5). Pe: Pego; Va:
843 Valencia; Am: Amenara; Ed: Ebro Delta; Cu: Cubelles; Ll: Llobregat Delta; Em: Empuries, Al: Alcudia; Gr:
844 El Grau.
845
846 Figure 4. RSL reconstructions in northern Corsica (4) and Sardinia (5) regions. SLIPs (boxes) are plotted as
847 calibrated ages against change in sea level relative to present. Limiting points are plotted as terrestrial or
848 marine horizontal lines. The dimensions of boxes and lines for each point are based on elevation and age
849 errors. Black lines denote the geography of relative sea-level predictions calculated using SELEN and
850 adopting the ICE-6G (VM5a) GIA model (see section 5). Cc: Cap Corse; Cf: Cala Francese; Sc: Scandola;
851 Sl: Sale lagoon; Sa: Sagone; Tg: Tanghiccia; Cv: Cavallo Island; Bs: Bonifacio Strait; Mj: Mignataghja; Ps:
852 Posada; Ca: Capo Caccia; Cl: Cala Liberotto; Or: Gulf of Oristano; Tb: Terralba; At: Sant`Antioco; Mf:
853 Capo Malfatano-Piscinni; Nr: Nora; Cg: Cagliari.
854
855 Figure 5. A) Top: 4th-order polynomial fits of the Balearics (blue, region 2) and Sardinia (red, region 5)
856 SLIPs. Bottom: Difference between the two fitted RSL curves through time, in metres. B) GIA sea-level
857 fingerprints for 2040–2050 relative to 1990–2000 in the Mediterranean Sea (modified from Galassi and

Spada, 2014). Predictions were obtained by SELEN (Spada and Stocchi, 2007), using models ICE-5G (VM2) (a, Peltier, 2004) and KL05 (b, Lambeck et al., 1998, Lambeck and Purcell, 2005).

Appendix A: SLIPs and limiting points included in the Relative Sea Level database. Latitude and Longitude are expressed in decimal degrees.

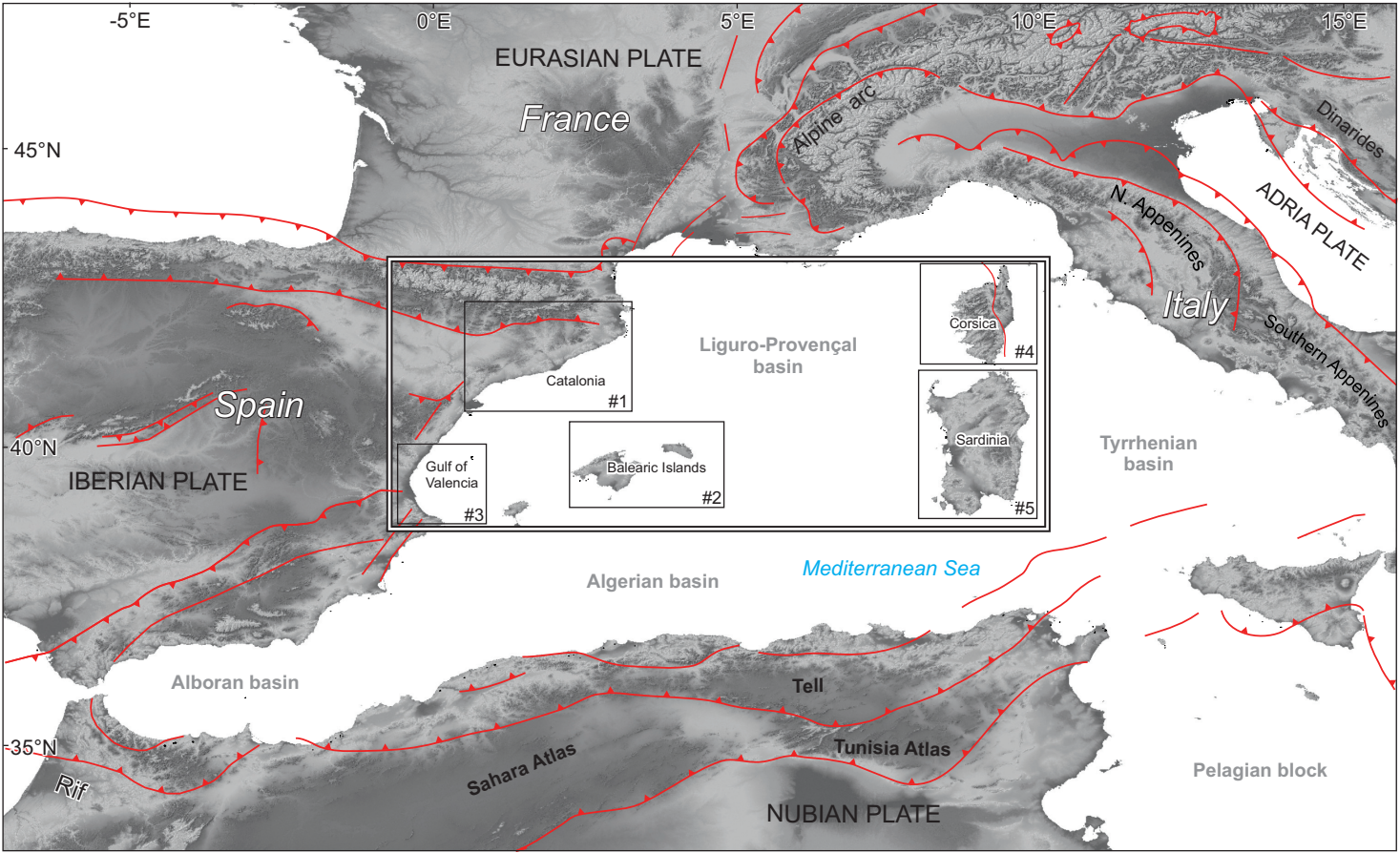
-5°E
0°E
5°E
10°E
15°E
45°N
40°N
35°N
EURASIAN PLATE
France
Alpine arc
Dinarides
ADRIA PLATE
N. Appenines
Italy
Southern Appenines
Spain
IBERIAN PLATE
Liguro-Provençal basin
Catalonia
#1
Gulf of Valencia
#3
Balearic Islands
#2
Corsica
#4
Sardinia
#5
Tyrrhenian basin
Mediterranean Sea
Algerian basin
Alboran basin
Tell
Tunisia Atlas
Sahara Atlas
Rif
NUBIAN PLATE
Pelagian block

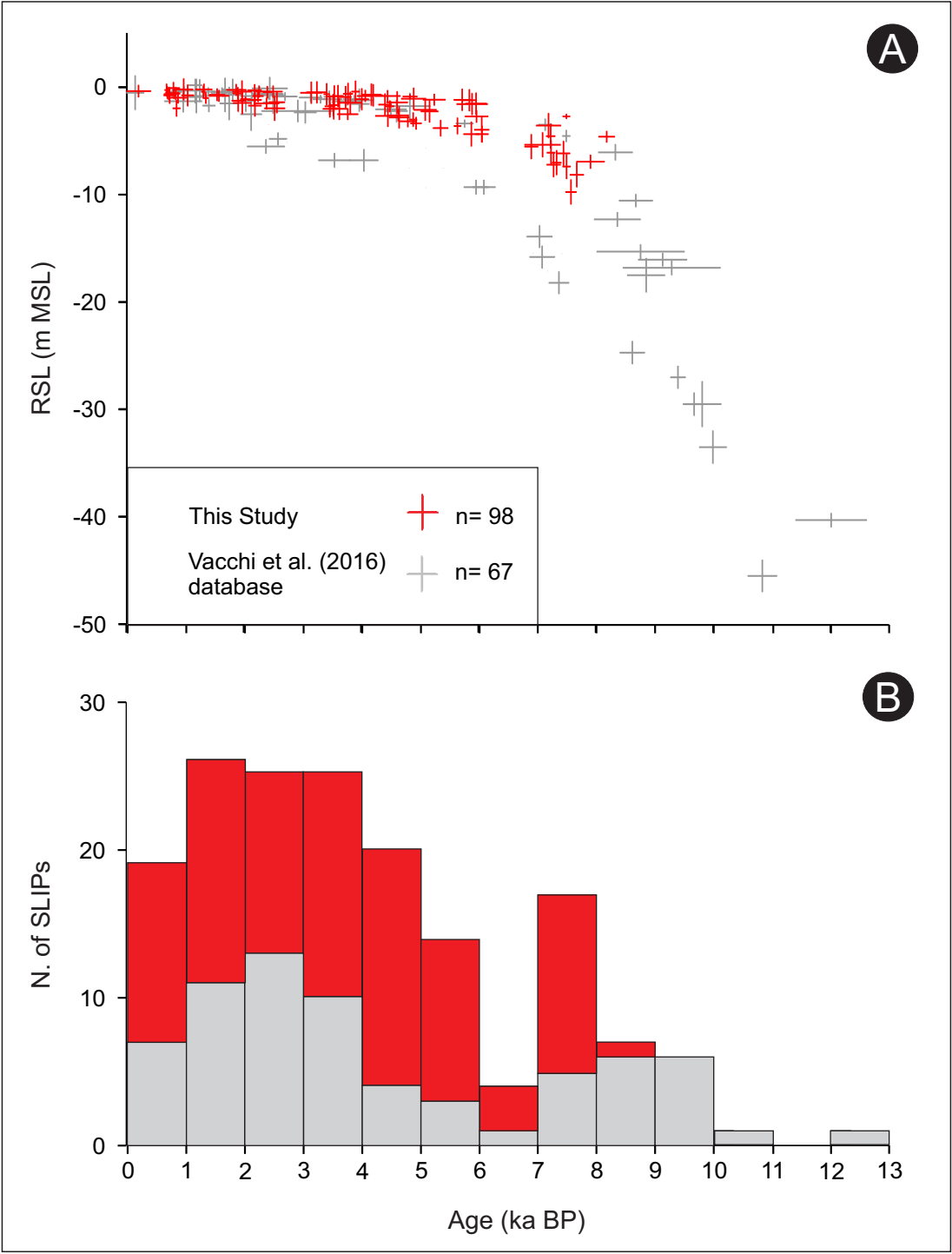
A
0
-10
-20
-30
-40
-50
RSL (m MSL)
This Study
n= 98
Vacchi et al. (2016) database
n= 67
B
30
20
10
0
N. of SLIPs
0
1
2
3
4
5
6
7
8
9
10
11
12
13
Age (ka BP)

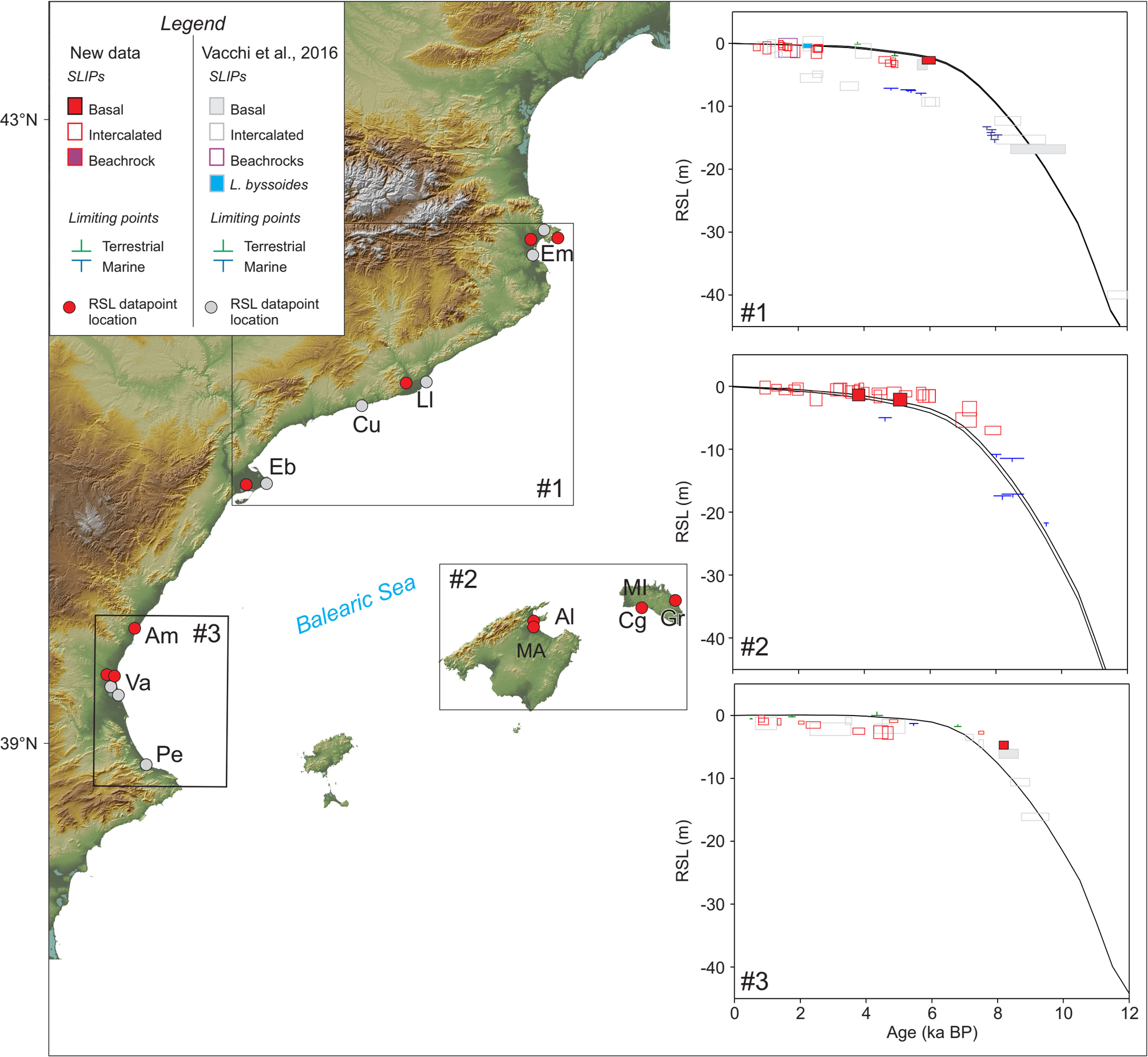
Legend
New data
SLIPs
Basal
Intercalated
Beachrock
Limiting points
Terrestrial
Marine
RSL datapoint location
Vacchi et al., 2016
SLIPs
Basal
Intercalated
Beachrocks
L. byssoides
Limiting points
Terrestrial
Marine
RSL datapoint location
43°N
39°N
Em
Ll
Cu
Eb
#1
Balearic Sea
#2
Al
MA
Ml
Cg
Gr
Am
#3
Va
Pe
RSL (m)
0
-10
-20
-30
-40
#1
#2
#3
0
2
4
6
8
10
12
Age (ka BP)

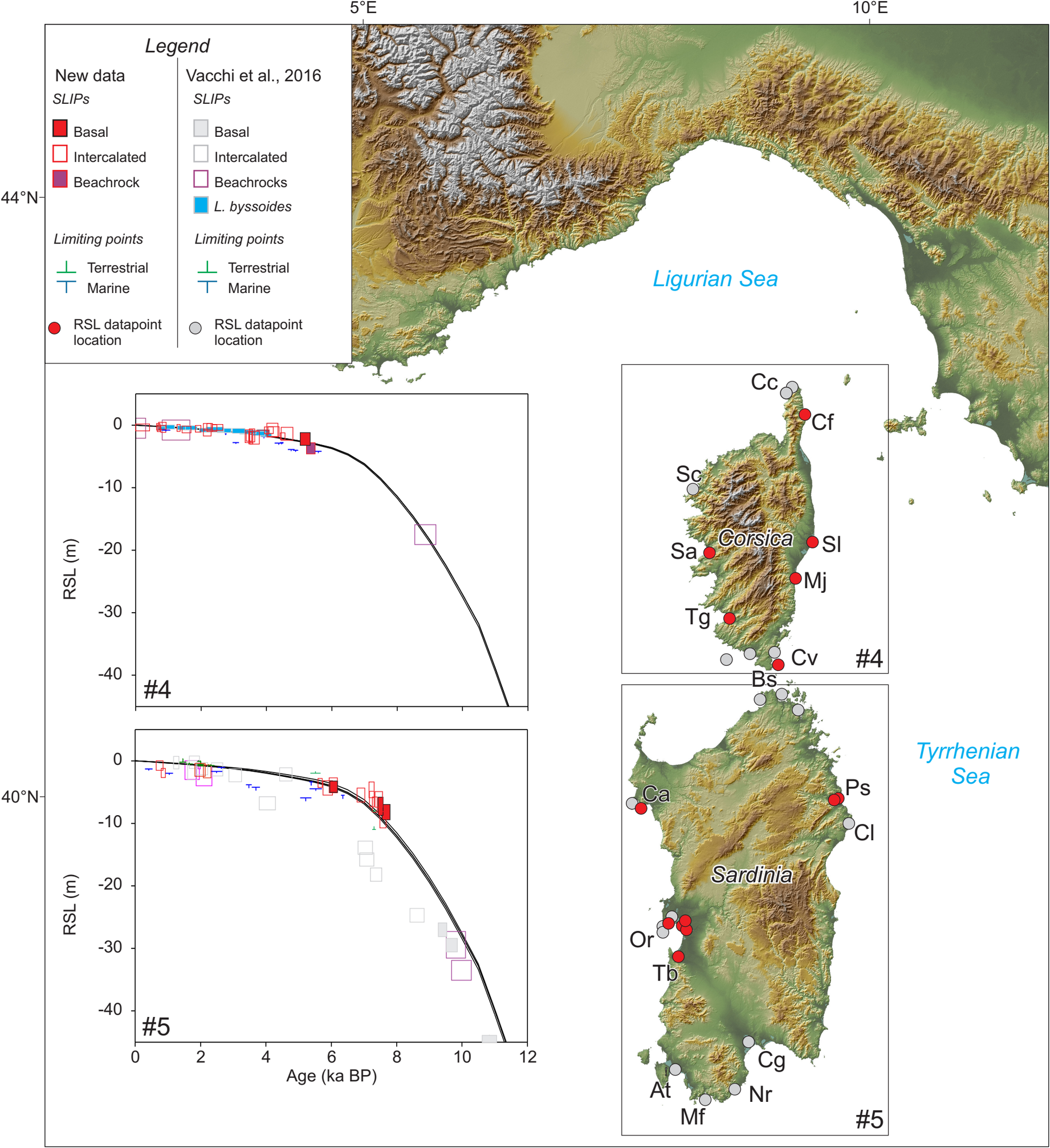
5°E
10°E
44°N
40°N
Legend
New data
SLIPs
Basal
Intercalated
Beachrock
Limiting points
Terrestrial
Marine
RSL datapoint location
Vacchi et al., 2016
SLIPs
Basal
Intercalated
Beachrocks
L. byssoides
Limiting points
Terrestrial
Marine
RSL datapoint location
Ligurian Sea
Tyrrhenian Sea
Corsica
Sardinia
Cc
Cf
Sc
Sa
Sl
Mj
Tg
Cv
Bs
Ca
Ps
Cl
Or
Tb
Cg
At
Nr
Mf
#4
#5
RSL (m)
0
-10
-20
-30
-40
0
2
4
6
8
10
12
Age (ka BP)

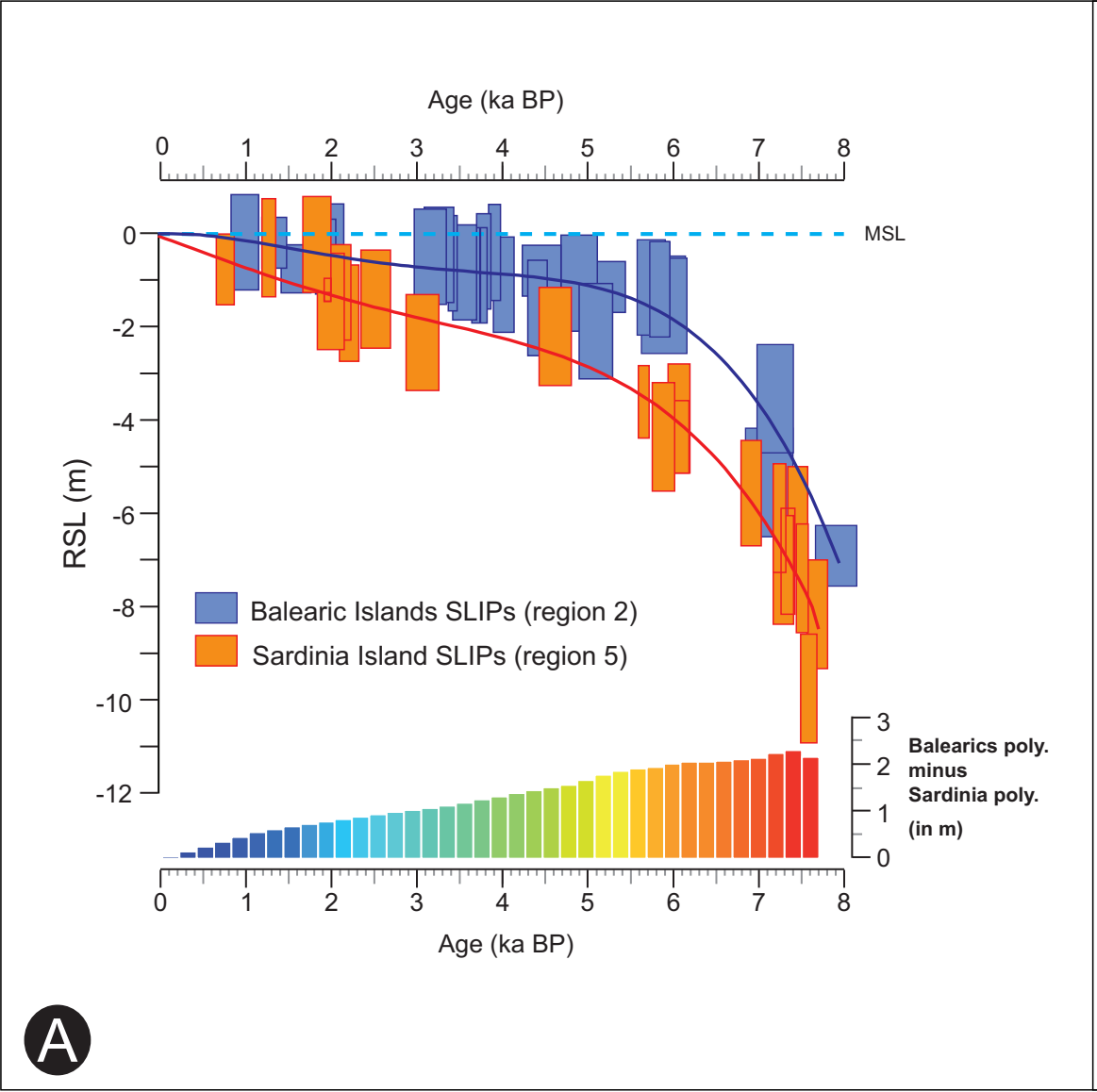
Age (ka BP)
0
1
2
3
4
5
6
7
8
MSL
RSL (m)
-2
-4
-6
-8
-10
-12
Balearic Islands SLIPs (region 2)
Sardinia Island SLIPs (region 5)
3
2
1
0
Balearics poly.
minus
Sardinia poly.
(in m)
Age (ka BP)
A

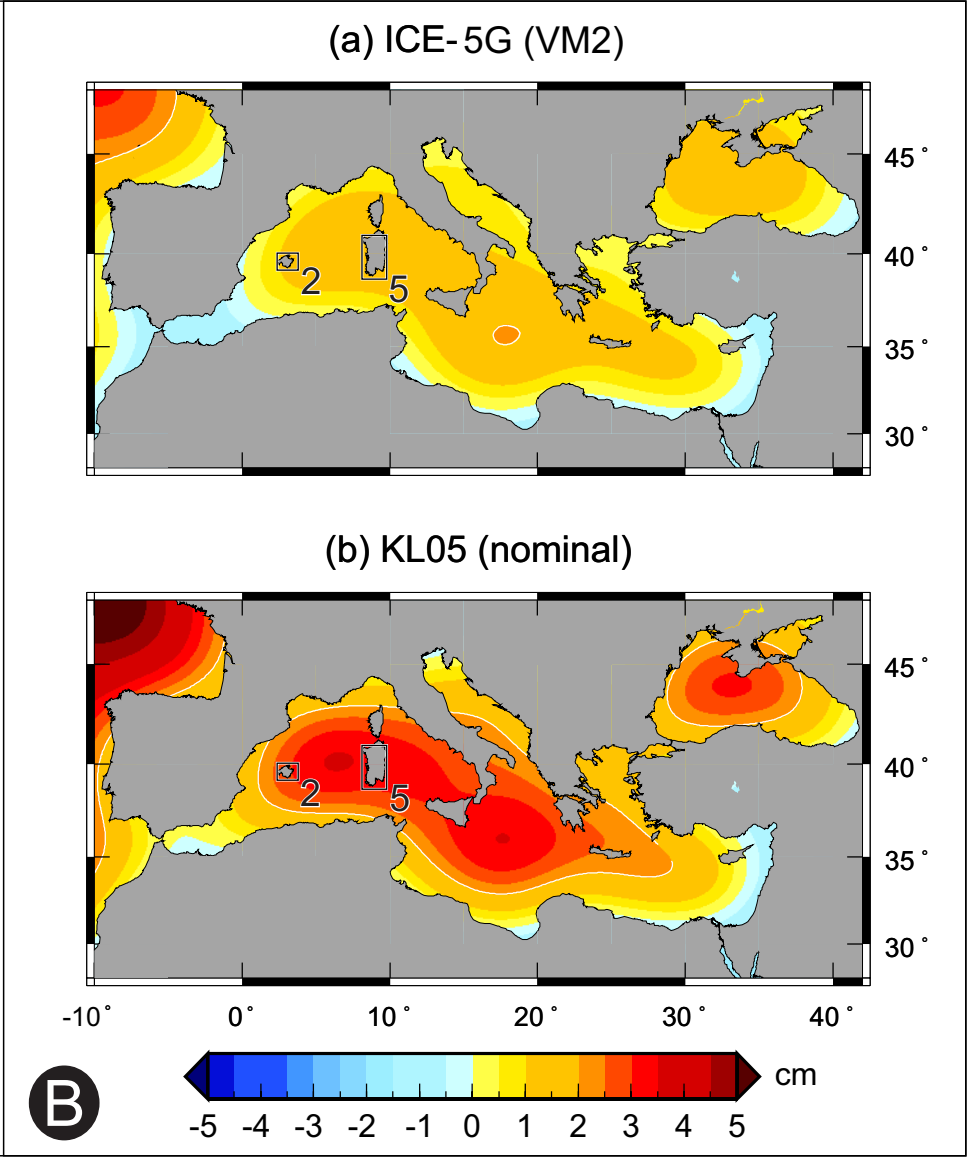
(a) ICE-5G (VM2)
2
5
45 °
40 °
35 °
30 °
(b) KL05 (nominal)
2
5
45 °
40 °
35 °
30 °
-10 °
0 °
10 °
20 °
30 °
40 °
cm
-5 -4 -3 -2 -1 0 1 2 3 4 5
B

Table 1. Summary of the indicative meanings used to estimate the relative elevation of the sea-level index points (SLIPs) and limiting points for the database (see Vacchi et al., 2016 for the detailed facies descriptions). HAT: Highest Astronomical Tide; MHW: Mean High Water; MLW: Mean Low Water; MSL: Mean Sea Level. Note that the investigated coastal sectors have a lower microtidal regime. HAT values are equivalent to the Mean Highest High Water and typically do not exceed 0.05 m above MHW. Similarly, the Mean Lowest Low Water values are equivalent to the MLW.

Sample Type	**Evidence**	**Reference Water Level**	**Indicative Range**
SLIPs			
***Lithophyllum byssoides* rim**	Identifiable *in situ* coralline rhodophyte *Lithophyllum byssoides* (formerly known as *Lithophyllum lichenoides*) recognized at species level (Laborel et al. 1994; Faivre et al., 2013).	(HAT to MSL)/2	HAT to MSL
Salt-marsh	Salt-marsh plant macrofossils (e.g. Vella et al., 2005; Di Rita et al., 2010, Primavera et al., 2011). Foraminiferal assemblages dominated by saltmarsh taxa (e.g., Caldara and Simone, 2005; Shaw et al., 2016, Cearreta et al., 2016).	(HAT to MSL)/2	HAT to MSL
Open or marine influenced lagoon	Macrofossil taxa dominated by marine brackish molluscs with the presence of *Cerastoderma glaucum, Bittium recticulatum* often associated with *Cerithium vulgatum* and *Loripes lacteus* (e.g. Di Rita et al., 2011; Giaime et al., 2017, Melis et al., 2018). Foraminiferal and ostracods assemblages dominated dominated by marine brackish littoral taxa or outer estuary taxa (e.g., Marriner et al., 2012b; Carmona et al., 2016; Salel et al., 2016). Higher species diversity compared to the semi-enclosed lagoon system.	-1 m	MSL to -2 m
Inner or semi enclosed lagoon	Macrofossil taxa dominated by brackish molluscs typical of sheltered marine-lacustrine environments with the presence of *Cerastoderma glaucum, Abra segmentum,* Hydrobbiidae spp. (e.g. Marriner et al., 2012b, Sabatier et al., 2012; Ghilardi et al., 2017a,b;). Foraminifera and ostracod assemblages dominated by brackish littoral taxa or inner estuarine taxa (Ejarque et al., 2016; Salel et al., 2016, Cearreta et al., 2017). Lower species diversity compared to the open lagoon system.	-0.5 m	MSL to -1 m

Undifferentiated brackish environment	Foraminiferal, diatom and ostracod assemblages dominated by freshwater-slightly brackish or swamp taxa and shallow marine taxa (e.g. Amorosi et al., 2013; Ghilardi et al., 2017a,b).	(HAT to MLW)/2	HAT to MLW
Beachrock with cement fabric or stratigraphic information	Samples showing intergranular intertidal cements (i.e., irregularly distributed needles or isopachous fibres of aragonitic cement or isopachous rims (bladed or fibrous) and micritic High-Mg Calcite cement e.g. Vacchi et al., 2012; Mauz et al., 2015)	(HAT to MLW)/2	HAT to MLW
General beachrock	Samples that do not meet the above requirements for a classification as intertidal beachrocks (e.g., Vacchi et al., 2016)	0.5 m	-1 to +2 m MSL
Limiting Points			
Marine limiting	Identifiable marine shells in poorly to well-bedded sandy and silty sediments typical of the upper shoreface or prodelta environments (e.g., Sabatier et al., 2012; Marriner et al., 2012b). *Posidonia oceanica* beds found in inner bay and shoreface marine deposits (Vacchi et al., 2017; Pascucci et al., 2018). Foraminiferal and ostracod assemblages dominated by marine taxa (Carboni et al., 2002; Rossi et al., 2011 ; Amorosi et al., 2013, Salel et al., 2017).	MSL	Below MSL
Terrestrial limiting	Freshwater plant macrofossils and peat with freshwater diatoms (e.g. Di Rita et al., 2010; Melis et al., 2016). Upper beach/foreshore deposits and terrestrial paleosoils. Foraminiferal and ostracod assemblages dominated by freshwater taxa in swamps or fluvial environments (Carboni et al., 2002; Rossi et al., 2011; Salel et al., 2016).	MSL	Above MSL